Designing Surface-enhanced Raman Scattering (SERS) Platform Beyond Hotspot Engineering: Emerging Opportunities in Analyte Manipulations and Hybrid Materials

Hiang Kwee Lee,[1,+] Yih Hong Lee,[1,+] Charlynn Sher Lin Koh,[1] Gia Chuong Phan-Quang,[1] Xuemei Han,[1] Chee Leng Lay,[1,2] Howard Yi Fan Sim,[1] Ya-Chuan Kao,[1] Qi An,[1,3] Xing Yi Ling[1,*]

Affiliations:

[1] Division of Chemistry and Biological Chemistry, School of Physical and Mathematical Sciences, Nanyang Technological University, 21 Nanyang Link, Singapore 637371.

[2] Institute of Materials Research and Engineering, Agency for Science, Technology and Research (A*STAR), 2 Fusionopolis Way, Innovis, #08-03, Singapore 138634.

[3] Beijing Key Laboratory of Materials Utilization of Nonmetallic Minerals and Solid Wastes, National Laboratory of Mineral Materials, School of Materials Science and Technology, China University of Geosciences, Beijing, China 100083.

[+] These authors contributed equally to this work.

*Correspondence to: xyling@ntu.edu.sg

Table of Contents

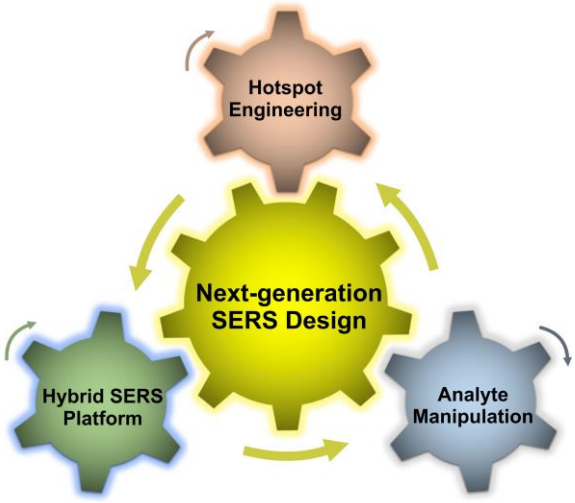

This review summarizes recent SERS developments, focusing on analyte manipulation strategies and hybrid SERS platforms that venture beyond hotspot engineering.

Key Learning Points

- Designing 0D/1D hierarchical particles, 2D metacrystals and 3D plasmonic open-structures are critical for efficient SERS hotspot engineering.
- In addition to hotspot engineering, analyte manipulation techniques and hybrid SERS platforms are emerging strategies to realize ultrasensitive SERS detection for analytes with no specific affinity to plasmonic surfaces.
- Chemical coupling approaches and chemical analyte directing strategies improve SERS detection by boosting the Raman cross-sections of weak Raman scatterers and capturing them near plasmonic surfaces, respectively.
- Functionalizing SERS platforms with non-wetting properties or porous materials physically concentrates analytes directly over electromagnetic hotspots, especially for gaseous or volatile liquid analytes with no affinity to plasmonic surfaces.
- Coupling plasmonic structures with secondary functional materials such as graphene, semiconductor nanoparticles, and piezoelectric materials yields hybrid SERS platforms with enhanced electromagnetic and chemical properties.

Abstract

Surface-enhanced Raman scattering (SERS) is a molecule-specific spectroscopic technique with diverse applications in (bio)chemistry, clinical diagnosis and toxin sensing. While hotspot engineering has expedited SERS development, it is still challenging to detect molecules with no specific affinity to plasmonic surfaces. With the aim of improving detection performances, we venture beyond hotspot engineering in this tutorial review and focus on emerging material design strategies to capture and confine analytes near SERS-active surfaces as well as various promising hybrid SERS platforms. We outline five major approaches to enhance SERS performance: (1) enlarging Raman scattering cross-sections of non-resonant molecules via chemical coupling reactions; (2) targeted chemical capturing of analytes through surface-grafted agents to localize them on plasmonic surfaces; (3) physically confining liquid analytes on non-wetting SERS-active surfaces and (4) confining gaseous analytes using porous materials over SERS hotspots; (5) synergizing conventional metal-based SERS platforms with functional materials such as graphene, semiconducting materials, and piezoelectric polymers. These approaches can be integrated with engineered hotspots as a multifaceted strategy to further boost SERS sensitivities that are unachievable using hotspot engineering alone. Finally, we highlight the remaining challenges and suggest new research directions toward efficient SERS designs critical for real-world applications.

1. Introduction

Surface-enhanced Raman scattering (SERS) is a non-invasive spectroscopic technique that utilizes unique molecular vibrational fingerprints to identify and quantify analytes down to ultratrace levels (Figure 1a).[1, 2] However, the Raman signals of most molecules are inherently weak due to their significantly smaller Raman scattering cross-sections compared to fluorescence cross-sections. To boost Raman signals, SERS employs plasmonic nanostructures made up of Ag, Au, Cu, and recently Al,[1] whereby the collective oscillation of the metal's conduction band electrons upon light excitation gives rise to localized surface plasmon resonances (LSPRs). Coupling of LSPRs with incoming light leads to a secondary electric field localized around the plasmonic nanostructures, generating plasmonic hotspots which effectively concentrate electromagnetic fields at/near the metallic surfaces (<10 nm) by 10^2-10^5-fold.[1, 2] This enhanced electromagnetic field amplifies both excitation and emitted radiations, with the resulting SERS intensity scaling according to the fourth power of field enhancement.[2] More importantly, such enhancement is independent of the nature of analyte molecules. This phenomenon is also known as the electromagnetic (EM) mechanism of SERS enhancement, and is the main contributor towards SERS signal enhancement in the range of 10^3-10^8-fold (Figure 1a).[1] Notably, the strength of electromagnetic fields can be tuned by modulating nanostructure morphology, dielectric functions, and/or interparticle plasmonic coupling to generate electromagnetic hotspots among neighboring particles. Besides EM enhancement, SERS can also be enhanced up to 10^3-fold via a chemical mechanism (CHEM).[1] Because CHEM arises from the enhanced polarizability (and hence SERS signals) between analytes and metallic surfaces,[2] this enhancement mechanism depends strongly on the analytes' chemical nature and analyte-surface interactions/affinity. Consequently, CHEM's applicability is restricted to a narrower range of chemical species such as thiolated molecules. Nevertheless, both enhancement mechanisms require analyte molecules to be in the proximity of plasmonic surfaces. A combined utilization of EM and CHEM mechanisms are essential for SERS to achieve ultratrace detection with sensitivity comparable to fluorescence spectroscopy.

Two important metrics are widely employed to quantify the overall SERS enhancement arising from EM and CHEM, namely enhancement factor (EF) and analytical enhancement factor (AEF).[1, 3] EF (Equation 1) quantifies signal enhancement by comparing SERS and normal Raman scattering (NRS) signal intensity (I), which is a useful parameter to benchmark SERS and the average field enhancement experienced by each molecule across different platforms. Accurate determination of number of molecules (N) measured within the laser confocal volume is required for this metric.

$$EF = (I_{SERS}/N_{SERS})/(I_{NRS}/N_{NRS}) \quad \text{(Equation 1)}$$

On the other hand, AEF (Equation 2) approaches signal enhancement from an analytical point-of-view, relating signal intensity to analyte concentration (C) rather than number of molecules.

$$AEF = (I_{SERS}/C_{SERS})/(I_{NRS}/C_{NRS}) \quad \text{(Equation 2)}$$

This metric is especially useful when it is hard to estimate the number of analyte molecules present, especially for analytes with no specific affinity to the plasmonic surfaces.

Motivated by the potentially gigantic signal enhancement achievable for the detection of diverse analyte species, various hotspot engineering strategies targeting EM mechanism have emerged over the years. These strategies include developing zero-/one-dimensional (0D/1D) plasmonic nanostructures exhibiting strong field confinement, as well as multi-dimensional (2D/3D) platforms with extensive plasmonic coupling to achieve large-area hotspots.[4] Moreover, new analytical techniques have been developed using the principle of hotspot engineering. Prominent examples include tip-enhanced Raman spectroscopy (TERS) and shell-isolated nanoparticle-enhanced Raman spectroscopy (SHINERS),[2, 5] both of which allow ultrasensitive single-molecule detection with sub-diffraction-limit spatial resolution. This ensemble of benefits gives SERS a competitive edge over other state-of-the-art spectroscopic/chromatographic detection methods, where the latter typically suffers from non-molecule-specific readout, poor sensitivity, and/or strict sample requirements.[6] It is therefore not surprising that SERS has evolved into a multi-disciplinary analytical approach that is widely employed in diverse fields, including mechanistic investigations in (bio)chemical reactions,[6, 7] clinical diagnosis,[8, 9] and environmental/food/industrial surveillance with attomolar detection limits.[3, 10-12]

Despite significant progress in developing efficient SERS platforms, majority of current SERS platform studies still utilize surface-grafted molecules or dye species as Raman probes for proof-of-concept demonstrations.[3, 13, 14] These molecules exhibit specific affinity to plasmonic surfaces and/or possess larger intrinsic Raman cross-sections, which may not be representative of analytes in practical situations. This scenario inevitably leads to questions such as "how do these state-of-the-art SERS platforms perform towards analytes with no/poor affinity to plasmonic surfaces and/or analytes that are poor Raman scatterers?" Indeed, it remains a formidable challenge to detect molecules that do not interact with/adsorb onto plasmonic surfaces, which is especially problematic for gaseous analytes owing to their low concentration and high mobility. This issue severely hinders the widespread adoption of SERS in practical applications because even the most optimally designed SERS platforms are essentially nullified if the target analytes cannot access the electromagnetic hotspots.

It is therefore critical to venture beyond hotspot engineering to overcome the current performance bottlenecks in SERS, with the eventual goal of transcending SERS from laboratory-based research into tackling real-world problems. In this review, we identify several promising and emerging material design strategies that can be easily integrated with current SERS platforms. These strategies can be categorized into two general concepts, which focus on (1) analyte manipulation and (2) creating multifunctional hybrid SERS platforms.

Efficient analyte manipulation improves the SERS detection of analytes (Figure 1b), especially for molecules with no specific affinity to the plasmonic surfaces and/or having low Raman cross-sections. In this approach, we discuss the problems associated with poor analyte affinity to the plasmonic surface, as well as innovative approaches to confine analytes near electromagnetic hotspots and SERS-active regions for optimal SERS sensitivity and signal reproducibility. Emerging analyte manipulation strategies include (1) using chemical interactions to capture and/or direct analyte molecules to functional plasmonic surfaces,[15, 16] (2) physically confining analytes close to the SERS-active region,[17, 18] as well as (3) encapsulating plasmonic nanostructures with a secondary sorbent material to concentrate analytes directly over the electromagnetic hotspots.[8, 11] Moreover, we can also chemically modify analyte molecules to

enhance their intrinsic Raman cross-sections and in turn boost their corresponding SERS signals.[9, 19] Multifunctional hybrid SERS platforms involve integrating engineered plasmonic nanostructures with secondary functional materials.[12, 20] This integration enables a synergistic modulation of the chemical and electromagnetic properties of the resulting hybrid SERS platforms and/or analytes to achieve efficient SERS readout. These synergistic effects are notably present only in the hybrid SERS ensembles. Collectively, strategies in analyte manipulation and creating hybrid materials offer an attractive two-pronged approach to improve SERS sensitivity by $>10^3$-fold,[10, 12, 16, 17, 21] thereby addressing the limitations that cannot be solely resolved using traditional hotspot engineering. More importantly, this two-pronged strategy allows parallel development in individual research fields, which can subsequently converge to achieve multiplicative breakthroughs in SERS sensing. Despite their importance to SERS detection, there is a lack of a comprehensive review to summarize current analyte manipulation strategies and hybrid SERS platforms along with their potential to achieve ultrasensitive SERS sensing in practical situations.

In this tutorial review, we discuss the latest progress in the development of SERS platforms (Figure 1c), focusing on analyte manipulation strategies and emerging hybrid SERS platforms that venture beyond traditional hotspot engineering. We begin with a brief overview of electromagnetic hotspot engineering, highlighting emerging strategies to create novel 0D/1D hierarchical plasmonic structures and 2D/3D plasmonic metacrystals featuring unprecedented plasmonic properties and stronger field enhancement. Next, we discuss various emerging analyte manipulation strategies in SERS design in the last decade, focusing on the basic working principles, fabrication approaches, and their corresponding contributions in advancing SERS detection. We further explore the synergism of SERS platforms with emerging functional materials – such as 2D materials and semiconductors – to create next-generation hybrid ensembles with tailorable electromagnetic and/or chemical properties that directly impact SERS performances. We have also tabulated a non-exhaustive list of these various platforms in Table 1-3, with the goal of providing an easily accessible update on current research in this area. Finally, we conclude our discussion with a critical outlook to highlight potential opportunities in future material designs,

particularly toward efficient and analyte-selective SERS platforms. We hope these insights can stimulate further scientific/technological advancements in SERS and the entire analytical discipline, where the grand aim of single/few molecules detection in real-world samples is highly sought after in various environmental, industrial, biological, defense, chemical applications.

2. Hotspot engineering: traditional approaches and emerging strategies

Electromagnetic hotspot engineering occupies the center stage in SERS research, focusing on the design of materials and platforms to achieve intense light confinement at the nanoscale, straddling zero-dimensional (0D) to three-dimensional (3D) space. 0D approaches focus on creating designer nanoparticles with unique structural features to enhance hotspot densities at the single particle level, whereas multi-dimensional plasmonic platforms center on exploiting the extensive plasmonic coupling along x-, y- and/or z-axis to significantly boost hotspot intensities, as well as enable a more efficient utilization of SERS platforms within the 3D laser excitation volumes. The aim of this section is to provide a brief overview of the latest developments in hotspot engineering from 0D to 3D (Table 1).

2.1 Engineering hotspot in zero- and one-dimension (0D / 1D)

Research on 0D/1D hotspot engineering over the past several decades has focused on the synthesis of shape-controlled metallic nanoparticles (such as Au and Ag) with regions of large curvatures (Figure 2a).[2, 4] These regions exhibit the well-known 'lightning-rod effect',[1] generating the strongest electromagnetic field enhancements required to achieve strong SERS signals. Examples of such anisotropic nanoparticles include nanorods,[22] wires,[23] and highly symmetrical Platonic nanoparticles such as nanocubes and octahedra.[14] As synthetic protocols for noble metal nanoparticles mature, we have also witnessed the creation of increasingly sophisticated morphologies such as various star-like structures.[4] In addition to traditional plasmonic metals, Al-based nanoparticles are promising new alternative SERS-active materials owing to Al's relatively low costs, high earth abundance, and capability in supporting LSPRs spanning the deep-UV to the visible wavelengths.[24] For instance, aggregates of ~150 nm truncated

trigonal bipyramidal Al nanocrystals with dipolar resonance at 570 nm exhibit quantitative detection of single-stranded DNA down to 2 μM without needing any modification to either the DNA or the Al nanocrystals.[24]

Aside from synthesizing complex nanoparticle morphologies, post-synthetic morphological modifications of as-synthesized shape-controlled nanoparticles also serve as an appealing approach to enhance hotspot density and electromagnetic field strength on a nanoparticle (Figure 2a). These modifications can generally be classified into (1) additive and (2) subtractive systems; more importantly, they preserve the intrinsic crystallinity of the as-synthesized nanoparticles such that the quality (Q)-factor associated with nanoparticles' plasmon resonances remains high.[4]

Additive systems increase hotspot densities by selectively depositing additional plasmonic nanoparticles onto as-synthesized nanoparticle templates (Figure 2a).[25] For shape-controlled nanoparticles such as cubes and octahedra,[14] reaction conditions can be adjusted to direct particle deposition along the more reactive nanoparticle edges and vertices with lower surface atom coordination. At the same time, the larger curvatures of these regions imply stronger field confinement along the edges and vertices. This 'hotspot-over-hotspot' approach has been successfully demonstrated with the precise deposition of Au nanoparticles along the edges and vertices of single-crystalline Ag octahedra to form selective edge Au-deposited Ag octahedra (SEGSO; Figure 2b).[25] SEGSO generates 15-fold stronger local electromagnetic field enhancements along the Au-deposited edges than pure Ag octahedra at the laser excitation wavelength. Consequently, the single-particle SERS EF of SEGSO on a substrate reaches 1.1×10^5, which is 3- and 10-fold higher as compared to non-selectively Au deposited-Ag octahedra and pure Ag octahedra respectively.

On the other hand, subtractive systems enhance hotspot densities through controlled removal of surface atoms from the nanoparticle templates via etching reactions (Figure 2a).[23] This strategy typically increases the surface roughness of the nanoparticle templates, thus enabling more efficient coupling of surface plasmons with far-field light to create stronger and more homogeneous electromagnetic fields. For instance, etching Ag nanowires with smooth surfaces using a hydrogen peroxide/ammonia mixture

yields highly roughened wires which resemble 'beads-on-a-string' (Figure 2c).[23] Unlike the original smooth wires which only exhibits SERS-activity at the tips, the SERS activity of etched Ag nanowires extends uniformly across the entire length of a roughened wire and increases the SERS-active surface areas by more than 10-fold. The etched nanowires further exhibit ~2-fold stronger single-particle SERS EF of 6.4×10^4 on a substrate than their smooth counterparts throughout the entire length of the nanowires.

Indeed, thriving research in nanoparticle synthesis and modification has given rise to a library of diverse nanoparticle morphologies to substantially engineer hotspots and improve SERS performance at the single-particle level. Despite significant progress in optimizing nanoparticle design for hotspot engineering, these individual particles by themselves cannot serve as efficient SERS platforms owing to their limited nanometer-scale SERS-active areas as well as insufficient strength of electromagnetic hotspot for ultratrace sensing. Moreover, the hotspots are randomly distributed within colloidal dispersions,[7] potentially leading to inconsistent field enhancements and SERS signals upon interacting with analytes.

2.2 Two-dimensional (2D) hotspot engineering

Organizing plasmonic nanoparticles/nanostructures into ordered 2D arrays effectively introduces plasmonic coupling between neighboring nanoparticles to generate strong and consistent electromagnetic field enhancements, with functional areas up to centimeter-scale.[26] We will discuss both bottom-up and top-down approaches in this sub-section, covering the latest research developments in 2D hotspot design. Due to the space constraints, we will not be covering colloidal nanoparticle clusters in this tutorial review and interested readers can refer to relevant reviews cited here.[4]

2.2.1 Bottom-up approaches

Nanoparticle self-assembly is widely utilized in the bottom-up construction of 2D SERS platforms, and the interface between two immiscible fluids (such as liquid-air and liquid-liquid) is one of the most appealing techniques for the scalable organization of 2D nanoparticle metacrystals.[26] Nanoparticles

spontaneously adsorb to the interface to minimize the interfacial free energy, resulting in the formation of building block morphology-dependent close-packed metacrystals.[22, 26] These metacrystals can be directly employed as substrate-less 2D SERS platforms for analyte detection at the soft liquid-liquid interface, notably without the need to transfer them onto a supporting substrate. For instance, Au nanorod assembly at the oil-water interface has enabled the simultaneous and quantitative detection of aqueous-soluble rhodamine 6G (R6G) and organic molecules such as oleic acid down to nanomolar level.[22]

Fluid-fluid interface also provides a versatile avenue to program nanoparticle organization, including the metacrystal lattice structure, interparticle spacing, and more importantly, the strength of electromagnetic field enhancements. A notable example here is the concept of 'one nanoparticle morphology, multiple superlattices' using shape-controlled nanoparticles such as Ag nanocubes and Ag octahedra (Figure 3).[26, 27] This concept modulates the hydrophilic/hydrophobic interactions between nanoparticle surfaces and both liquid phases to generate multiple distinct metacrystals using just one type of shape-controlled nanoparticle, including close-packed and progressively open structures. The use of noble metal nanoparticles as building blocks implies that the nanoparticles' surface wettabilities can be easily tuned using thiolated molecules possessing varying hydrophobicities. Notably, hexagonal arrays of standing Ag nanocubes with a low packing density of 24% can be assembled using hydrophobic nanocubes.[27] Despite its low packing density, total field enhancement of this hexagonal metacrystal is 26-fold stronger than the square close-packed array on a substrate (100% packing density), leading to 350-fold higher SERS EF relative to the square close-packed array at the laser excitation wavelength. This study evidently demonstrates the importance of metacrystal engineering and that "more is not always better", thus challenging the traditional notion of squeezing the maximum number of nanoparticles into a fixed volume to achieve higher SERS efficiency.

2.2.2 Top-down approaches

Parallel to the development of bottom-up approaches is top-down lithographic techniques, including but not limited to e-beam lithography, photolithography, and nanoimprint lithography.[4] These fabrication

techniques allow precise control over hotspot locations and structural geometries on a substrate, achieving strong and spatially defined electromagnetic field distributions. Advances in fabrication techniques have enabled the fabricated nanostructure morphology to progress from traditional bow-tie configurations into increasingly complex structures. Moreover, precise structural control afforded by lithographic fabrication gives rise to unprecedented optical phenomena such as the Fano resonance in an array of heptameric nanoparticle clusters,[4] which is a non-radiative plasmon mode generating the strongest field enhancements around and within the cluster. Consequently, largest SERS enhancements are achieved when the excitation laser and the Stokes mode of interest overlap with the Fano resonance wavelength. However, a shortcoming of this platform is that a slight spectral mismatch between the Fano resonance and the Stokes mode/excitation wavelength (caused by changes in cluster sizes or gap distances) can lead to significantly lower SERS signals, thus placing stringent demands on the fabrication protocol. The discussion thus far certainly highlights the advantages of both bottom-up and top-down approaches: nanoparticle self-assembly presents a viable route for scalable metacrystal and 2D hotspot engineering while lithographic fabrication enables precise architectural control for optimal electromagnetic field enhancements.

Given the success of both top-down and bottom-up techniques in 2D hotspot engineering, it is hardly surprising that integrated approaches combining these two strategies have emerged to harness their respective advantages in fabricating high-performance SERS platforms. Aside from the more well-established nanosphere lithography, employing lithographically-fabricated templates in nanoparticle self-assembly allows the creation of targeted particle clusters with uniform and spatially-defined hotspots.[4] For instance, various clusters of shape-controlled Ag polyhedra can be assembled into pre-defined templates in high yields, with the cluster geometry and size dependent on the template dimensions. In clusters assembled using nanocubes and octahedra, SERS EF increases from $10^3 – 10^4$ to $10^6 – 10^7$ as the cluster sizes increase from monomers to teramers (12-mers).[28]

Another emerging integrated approach to create 2D SERS platforms with well-defined particle structures and clusters is direct metal writing using two-photon lithography. This strategy typically utilizes a high-energy ultrafast laser pulse for localized and in-situ reduction of metallic precursors into metal

nanoparticles, achieved by piezo-controlled raster scanning of the laser pulse within a droplet of photoresist on a substrate.[29] Pre-defined arrays of SERS-active microstructures comprising densely packed metal nanoparticles can be attained, with particle density reaching 1000 particles/μm^2 and SERS EF reaching 3×10^5. A major advantage of direct metal writing is its ability to realize remote and precise hotspot engineering, including the fabrication of well-defined plasmonic structures within microfluidic channels for real-time monitoring of volatile organic compounds.[29] The integration of top-down and bottom-up techniques therefore effectively empowers precise and high throughput hotspot engineering while eliminating the need for sophisticated protocol/equipment, high cost and long fabrication duration. However, a significant shortcoming of these engineered 2D hotspots is the under-utilization of the 3D confocal volume of the laser irradiation, limiting SERS sensitivity and requiring precise laser focusing due to a low tolerance for focal misalignment.

2.3 Engineering hotspots in three-dimensions (3D)

Efficient utilization of the 3D laser excitation volume, which typically extends over micron-sized dimensions in all three Cartesian planes, is essential to achieve optimal SERS performance. Within the excitation volume, the hotspot densities and effective exposed SERS-active areas can critically impact the corresponding intensity of the SERS signals. 3D SERS platforms overcome the limitations of 2D SERS platform through enhanced utilization of the entire laser excitation volume. There is also increased tolerance to laser misfocus along the z-plane, where sufficient hotspots remain within excitation volume to generate consistent SERS signals. Currently, 3D SERS platforms are mainly created via the self-assembly of colloidal nanoparticle building blocks into various large-area 3D structures and close-packed supercrystals demonstrated.[14] Building block morphology typically controls the lattice structures and consequently, the particle arrangements as well as electromagnetic field distributions among these supercrystals. However, the close-packed nature of these supercrystals inhibits effective penetration of excitation laser and analytes into the internal bulk supercrystal, as well as hinders the efficient collection of Raman scattered light from the internal bulk regions.[30] SERS measurements conducted using close-

packed woodpile arrays of Ag nanowires on a Si substrate clearly illustrate this point, whereby SERS signals plateau at the third particle layer with a constant full-width half-maximum (FWHM) intensity-depth profile of 1.3 μm.[30]

Consequently, research in 3D hotspot engineering has steered towards designing open structures to improve accessibility of both light and target molecules to the interior bulk for maximum SERS responses. Indeed, hyperspectral SERS imaging of an open 3D Ag nanowire mesh-like array on a Si substrate reveals improved FWHM of the intensity-depth profiles at ~ 15.8 μm.[10] Furthermore, non-close-packed allotropic arrays of Au nanoparticles obtained via the selective etching of Fe_3O_4 nanoparticles in a binary nanocrystal superlattice comprising Au and Fe_3O_4 building blocks demonstrate enhanced analyte diffusion into the crystalline lattices (Figure 4a, b).[31] More recently, multiple dual-structure 3D supercrystals are formed through the self-assembly of shape-controlled Ag polyhedra in two distinct micro-environments, driven by a combination of minimizing interfacial energy and hard particle interactions.[14] Featuring open structures atop densest-packed supercrystals, these dual-structure supercrystals demonstrate an additional 3.3-fold enhancement in SERS EF as compared to uniform densest-packed supercrystals on a substrate (5.2×10^6 versus 1.6×10^6; Figure 4c, d).

Integrated approaches combining top-down and bottom-up techniques have also been utilized to create open 3D SERS platforms. One approach uses polymeric films dewetting and phase-separating in nanoimprint molds to form highly porous microcylindrical templates, followed by electrostatic self-assembly of metallic nanoparticles to form open SERS-active microcylinders with SERS EF of 6.5×10^4.[13] When compared against a non-porous microcylinder template, the presence of 3D porosity on the microcylinders enables a higher loading of Au nanoparticles and enhances SERS signals by >10-fold. A separate study employing the assembly of Ag nanocube monolayers on photolithographically fabricated prism structures demonstrates how the prism's inclination angle can impact the strength of SERS signals in 3D;[32] experimentally determined optimum angle is 30° with a highest EF of 3.4×10^6. These research highlight the importance of 3D architecture design to efficiently access a higher density of engineered hotspots for stronger SERS activities.

An emerging strategy to fully utilize the 3D hotspot architecture involves miniaturized plasmonic liquid marbles and plasmonic colloidosomes,[3, 19] which are compact spherical millimeter-/micrometer-sized droplets featuring metal nanoparticles decorated surfaces (Figure 4e). Prepared by the spontaneous adsorption of colloidal plasmonic nanoparticles onto a liquid-liquid interface, the thicknesses of these particle-assembled microdroplets are easily tuned by regulating the amounts of nanoparticles added to the fluidic system prior to formation. Featuring thin but extended 3D networks of hotspots, both plasmonic liquid marbles and colloidosomes are substrate-less SERS platforms with high AEF between $10^6 – 10^8$,[3, 19] enabling their application in multiplex and multiphase ultratrace analyte detection. Moreover, the strong and reproducible SERS signals generated using plasmonic liquid marbles allow the monitoring of real-time kinetics of surface grafting reactions and interfacial protonation reaction.[6, 7]

Hotspot engineering has come a long way since the discovery of SERS on roughened electrodes. Our discussion here highlights some of the important new perspectives gained from recent research, including ways to synthesize designer nanoparticles, strategies to engineer metacrystals for efficient light confinement, and ways to utilize the laser's 3D excitation volume more efficiently. Nevertheless, two persistent problems still exists in the realm of hotspot engineering: (1) "is hotspot engineering alone sufficient to detect analytes with no/poor Raman activities, especially those involving monoatomic chemical species" and (2) "what about analytes with no specific affinities to the plasmonic surfaces, and hence cannot approach the SERS hotspots consistently?" In this case, we expect poor/negligible SERS responses even with the realization of the most intense and optimally engineered electromagnetic hotspots. Given that most studies still employ Raman probes that have affinity to the plasmonic surfaces and/or possess large Raman cross-sections, such scenario is indeed very real and frequently plagues SERS investigations, especially in practical analytical applications. As research in hotspot engineering continues to constitute a major focus towards ultrasensitive SERS readouts, we show in subsequent sections that SERS research has also branched out into various related disciplines that emphasize more on two unique perspectives – analyte manipulation strategies and creating hybrid material platforms.

3. Analyte manipulation: beyond hotspot engineering

In this section, we discuss on emerging concepts in manipulating analyte molecules to further boost SERS performance by 10 – 10^4-fold. The central goal here is to enrich local analyte concentration in the proximity of SERS-active plasmonic surfaces through various approaches, particularly for molecules with poor/no affinity to plasmonic surfaces. Three broad concepts will be discussed: chemical strategies that (1) enlarge molecular Raman cross-sections and/or (2) capture/direct analytes onto plasmonic surfaces, as well as physical strategy to (3) directly confine analyte over SERS-active surfaces (Table 2).

3.1 Enlarging molecular Raman cross-sections using chemical coupling approaches

The detection of small molecules remains a challenge owing to their low non-resonant Raman cross-section (~10^{-33} m^2) and lack of interaction with SERS-active plasmonic surfaces. The general approach to enlarge the low Raman cross-sections of molecules is to rationally modify the chemical structure through coupling reactions. This approach creates an electronic transition close to the laser-excitation frequency,[9, 19] resulting in resonance Raman scattering (RRS). Integrating RRS amplification with SERS leads to SE(R)RS, which has been demonstrated to efficiently boost Raman signals by 10^3-10^4-fold. In a model study using a plasmonic liquid marble platform, non-resonant environmental toxin bisphenol A (BPA, electronic transition at 280 nm, no affinity towards Ag) does not show any distinguishable SERS feature (Figure 5).[19] Coupling BPA with an aryl-diazonium cation yields colored molecules with absorption peak at 476 nm, giving rise to SER(R)S detection limits of 10 amol and a quantitative detection over a concentration range spanning 9 orders of magnitude. This detection limit is 50000-fold lower than the BPA safety limit and is >10^7-fold more sensitive than UV-vis absorption spectroscopy detection.

A similar diazonium coupling reaction has also been employed for the trace detection of various phenolic estrogens at sub-nanomolar levels in solution.[9] Rich vibrational fingerprints can be detected from these coupled molecules upon mixing and drying with Ag colloids, enabling rapid differentiation of related estrogens even in mixed solution. The advantage of this coupling strategy lies in its ease of use, where the coupling reaction and SERS measurement can be completed within 2 min at ambient

environment. This enables ultrasensitive detection of phenolic analytes in dilute solutions with high selectivity and at micro-liter volumes. However, the drawback of this approach is that its detection is limited to phenolic and aniline molecules. There is a need to develop other chemical reactions to effectively enhance the Raman cross-sections of weak Raman scatterers with different chemical functionalities. While the Raman scattering efficiency of these phenolic molecules are enlarged upon chemical reaction, they may still not be able to interact efficiently with plasmonic surfaces, especially when analytes are present at ultratrace level and/or exist as free/mobile molecules in liquid solvents.

3.2 Chemical analyte directing strategies

Chemical analyte directing strategies employ specific chemical interactions between nanoparticle surface-grafted chemical moieties and targeted functional groups on the analytes to selectively capture analyte molecules near plasmonic surfaces (Figure 6). The grafting species on the plasmonic surfaces typically possess affinity to metallic surfaces, ranging from small thiols and nucleic acids to extensive macromolecules. These species capture target analytes via various interactions ranging from weak non-covalent electrostatic interactions (250 kJ/mol) or hydrogen bonds (10-65 kJ/mol) to strong covalent (100-400 kJ/mol) or chelate bonds (0-400 kJ/mol).[33] These SERS platforms selectively capture target analytes from a complex sample matrix, thus reducing interfering signals and minimizing chances of false positives, which are commonly encountered during the analysis of complex samples. Two detection schemes will be discussed here: direct detection (based on vibrational fingerprints from target analyte) and indirect detection (based on SERS signals from labelling molecules).

3.2.1 Direct detection using designer plasmonic surfaces with analyte-capturing moieties

Direct detection enriches analyte concentration on plasmonic nanoparticle surfaces through specific chemical reactions between the target analyte and nanoparticle surface-grafted moieties (Figure 6a-i). Successful analyte detection relies on the elucidation of molecular vibrational fingerprints unique to the captured analyte molecules. This detection scheme is particularly useful for molecules with poor affinity

to plasmonic surfaces, and can further be categorized into passive and active setups. Passive direct detection largely depends on the diffusion of analyte molecules from the bulk phase to the particle vicinity for interaction. This detection has been applied to the quantitative sensing of chemical warfare simulants such as methylphosphonic acid (MPA) down to 1 ppb, using 2-aminoethanethiol-functionalized Au-coated Si nanocones (Figure 6a-ii).[34] Interaction between amino groups (-NH_2) of the surface thiols and the phosphonic groups (HO-P=O) of MPA results in the formation of a strong phosphoramide (N-P=O) bond, thereby enabling the detection of MPA molecules, which exhibit poor affinity towards unmodified metallic surfaces. This work offers an attractive method for molecular-level sensing of warfare chemicals and can be vital in national security/defense and anti-terrorism. Besides covalent bond formations, similar detection schemes have also been successfully demonstrated using non-covalent-based intermolecular interactions. These include electrostatic (-COO^-/–NR_4^+), hydrophobic (between aromatic rings), and hydrogen bonding interactions (-OH/-COOH/-NH_2) for the sensing of antidepressant/anticonvulsant drugs, polycyclic aromatic hydrocarbons, and glucose, respectively.[1] However, this method could be limited by slow and passive molecular diffusion. That is, the analyte capturing events and subsequent detection could be challenging at low analyte and/or plasmonic particle concentrations due to the lower probability of analyte-surface interactions/collisions.

Active direct detection overcomes issues arising from passive analyte diffusion to enable ultratrace analyte detection. This detection uses magnetic nanoparticles in combination with plasmonic nanoparticles to realize magnetic field-driven nanoparticle actuation within the colloidal dispersion, thus increasing the probability of interactions between target analytes and surface-modified plasmonic surfaces. For instance, nanocomposite particles comprising magnetite core and Ag shell with surfaces modified with iron nitriloacetic acid (Fe-NTA) enable SERS detection of dopamine via the formation of coordination bonds between dopamine's phenolic oxygen and Fe atoms on Fe-NTA.[15] In the presence of a moving magnet, vibrational fingerprints corresponding to dopamine remain observable even at femtomolar levels, translating to 10^5-fold enhanced sensitivity as compared to other dopamine detection platforms without the use of magnetic actuation. Notably, both the nanocomposites and captured analytes

can be easily separated from complex biological matrices such as cerebrospinal fluid and mouse striatum with the use of a static magnet, thus giving rise to potential applications in medical diagnosis. As an example, SERS detection of antibody immunoglobulin G (IgG) from a complex blood matrix can be achieved at $fg.mL^{-1}$ levels using highly selective host-guest interactions with anti-IgG-grafted nanoparticle surfaces followed by magnetic-assisted separation.[35] Active direct detection is therefore an appealing method to achieve ultrasensitive and interference-free detection of complex biological samples, bypassing multi-step separation processes typical in conventional bio-analytical methods such as electrophoresis and liquid chromatography.

3.2.2 Indirect analyte detection using plasmonic surface-grafted Raman molecular switch

Indirect SERS detection is a viable approach to sense analytes with weak vibrational fingerprints or inactive Raman vibrations, such as small molecules, gases, and monoatomic ions (Figure 6b-i).[16] This strategy grafts Raman labels onto the surfaces of plasmonic nanoparticles, which also serve as analyte capturing moieties. These labels typically exhibit strong characteristic Raman signals and possess functional group(s) for efficient interaction with the target analyte. Interactions between the analytes and Raman labels induce a change in the molecular configuration of the labels, in turn creating observable changes in the intensity and/or energy of SERS vibrations. In indirect SERS detection, we detect the presence of analyte using the changes to the Raman label's vibrational modes rather than the intrinsic molecular fingerprint of analyte. For instance, Au nanoparticles grafted with aromatic palladacycles function as turn-on sensors for the *in-vitro* detection of intracellular carbon monoxide (CO).[36] Upon introducing these SERS probes into living cells, intracellular CO molecules undergo carbonylation reaction with the surface-grafted palladacycle to yield a phenolic acid product, generating six new vibrational modes between 1000 and 1300 cm^{-1}. In a separate example on the detection of Raman-invisible chloride ions (Cl^-),[16] a chloride-sensitive organic fluorophore is grafted onto Ag surfaces deposited over micrometer-sized silica beads (Figure 6b-ii). π-π interaction between chloride anions and fluorophore's aromatic rings leads to geometrical and electronic changes to the latter, whereby increasing Cl^-

concentration increases the intensity ratio between ring stretching modes at 1497 and 1472 cm^{-1}. Quantitative non-destructive detection reaches picomolar levels, which is 10^3 – 10^6-fold more sensitive than common destructive methods of Cl^- sensing, such as ion chromatography and atomic absorption/emission spectroscopy.

Indeed, directing analytes towards plasmonic surfaces via various surface chemical modifications significantly enhances sensitivities towards analytes with poor Raman cross-sections and affinity to metal surface. However, such analyte directing strategies also suffer from several drawbacks, which should be taken into consideration in platform design. Grafting of Raman tags and recognition molecules onto plasmonic nanoparticle surfaces is non-trivial, involving multi-step reactions that are time-consuming (>12 hours). While chemical recognition creates high molecular selectivity due to specific interactions, these detection schemes can also introduce SERS interferences from Raman tags/recognition molecules and at the same time place stringent requirements on the reaction conditions as well as the type of applicable molecules. A more universal analyte capturing technique to actively accumulate target molecules near electromagnetic hotspots for ultrasensitive and widely-applicable molecular detection should be pursued.

3.3 Physical analyte concentrating strategies

Material designs to directly and physically concentrate target molecules to the SERS-active regions are promising because they are label-free, less/not dependent on analyte's chemical nature, and are essential for molecular detection especially at ultratrace concentration. We will discuss several effective physical analyte concentrating strategies to boost SERS enhancement for a wide range of molecules that do not exhibit specific affinity with the SERS platforms.

3.3.1 Molecular enrichment on non-wetting SERS platforms

Superhydrophobic SERS platforms can concentrate aqueous analytes within a small area,[17] representing a new prospect towards efficient detection of few molecules in highly diluted samples

(Figure 7a). In the absence of hydrophobic surface modification, common SERS substrates are generally hydrophilic where liquid samples spread across the substrate surfaces.[37] This is disadvantageous for trace detection because analyte spreading effectively dilutes the surface molecule concentration on the SERS substrate, in turn posing significant challenge in obtaining strong and reproducible SERS signals. Characterized by micro-/nanoscale surface roughness and hydrophobic chemical functionality, superhydrophobic SERS platforms display distinct water repelling properties with a water contact angle larger than 150^{o} and comparatively smaller solid-liquid contact area. Notably, superhydrophobic SERS substrates exhibiting Cassie-Baxter-type non-wetting phenomenon further improve analyte concentrating capabilities because the formation of air pockets at solid-liquid interfaces renders the platform with non-stick properties (lotus-like).[10, 17] This allows the liquid droplet to remain quasi-spherical during water evaporation, translating to an effective shrinking of the solid-liquid contact area for additional analyte enrichment. Analytes consequently precipitate within a highly confined area of several μm^2 on the SERS substrate, thereby concentrating analytes up to 10^4-fold and enabling detection limits down to attomolar (aM) regime.[17]

Superhydrophobic surfaces are widespread in nature, and have been utilized to create green SERS platforms. For instance, taro leaf surfaces are superhydrophobic with a static water contact angle of 154^{o}.[38] Hierarchical micro-/nanostructures comprising micro-papillae (~20 μm) and crossed secondary nanoplates on the leaf surfaces gives rise to Cassie-Baxter-type non-wetting behavior. Following the coating of 20-nm Ag to impart SERS activity, the taro-leaf@Ag platform concentrates a 4 μL R6G droplet within an area of 0.3 mm^2, corresponding to an analyte concentration factor of 43-fold as compared to hydrophilic surfaces (contact angle 30^{o}). Its detection limit reaches 10^{-8} M with high signal reproducibility (relative standard deviation <10% over >1200 measurements) and a corresponding EF of ~10^6. However, structural variations in naturally occurring templates may give rise to differences in batch-to-batch surface wettabilities, which in turn affect SERS sensitivities and reproducibility.

Both top-down and bottom up approaches have been employed to fabricate superhydrophobic SERS platforms with high structural fidelity and defined surface non-wettability. Top-down approach involves

fabricating non-metallic micro-/nanostructured surface through lithographic means,[17] followed by the physical deposition of Ag films on these pre-formed structures. For example, a Ag-decorated periodic array of silicon micropillar fabricated using optical lithography exhibits stable Cassie-Baxter superhydrophobicity with contact angle of ~160°.[17] A 40-fold reduction in droplet size occurs as the analyte droplet dries on the substrate, translating to an analyte concentrating factor of 10^4 when compared to conventional SERS substrate. Consequently, such superhydrophobic SERS substrate achieves detection of R6G down to 10 aM (~100 molecules) as well as successful detection of lambda DNA and lysozyme from solutions at atto- and femtomolar concentrations, respectively. While these achievements represent a significant breakthrough in nanosensor capabilities, chip fabrication is typically multistep and separates attaining superhydrophobicity from SERS-activity, that is, superhydrophobic non-SERS-active structures are first fabricated prior to imparting SERS-activity.

Bottom-up approaches directly organize well-defined crystalline plasmonic nanoparticles into large-area assemblies, thus eliminating the need of multistep fabrication protocol of top-down processes, and followed by surface chemical functionalization to achieve superhydrophobicity. The use of crystalline nanoparticles effectively boosts the local field enhancement as compared to the use of physically deposited polycrystalline Ag film, and potential Raman signal interference from non-metallic artificial and/or natural superhydrophobic templates are also minimized. The first report on bottom-up fabrication of superhydrophobic SERS platform utilizes the interfacial assembly of Ag nanocubes into a rough metallic array, followed by chemical surface modification with perfluorodecanethiol to render superhydrophobicity directly to the SERS substrate.[37] Modulating the nanocube density directly impacts the surface roughness of the platform, and the highest achievable advancing contact angle is 169°. When compared against a hydrophilic surface, this superhydrophobic SERS platform demonstrate 14-fold smaller spot sizes upon droplet drying. A detection limit of 10^{-16} M for R6G is achieved using just a 1-μL analyte solution, corresponding to an AEF of 10^{11}. Compared to Ag film-coated silica nanoparticle array, this platform exhibits 10^5-fold higher SERS performance, emphasizing the importance of utilizing single-crystalline Ag crystals for stronger field enhancement. This protocol is cost- and time-effective as

equipment and procedures required are simple and low-cost, thus creating great opportunities for high-throughput sensing of biomolecules, environmental toxins, and food additives. Nevertheless, a shortcoming of these substrates is their relative ineffectiveness in confining analytes dissolved in low-surface-tension organic liquids. This limitation implies that superhydrophobic SERS platforms are less efficient in detecting organic-soluble analytes, which are prevalent as food colorants and environmental contaminants.

To address this challenge, the fabrication of superhydrophobic-oleophobic SERS substrates featuring strong aqueous and organic liquid repellency along with superior SERS enhancement towards multiple analytes has been reported (Figure 7b-f).[10] The strategy involves the interfacial layer-by-layer assembly of Ag nanowires into 3D non-close-packed mesh-like arrays followed by chemical surface functionalization with perfluorodecanethiol. Contact angles of 170^{o} and 112^{o} are achieved for water and toluene (surface tension of 72.7 and 28.5 mN/m), respectively. These non-wetting phenomena consequently enrich both aqueous- and toluene-soluble analytes by ~100-fold and 10-fold, respectively. The lower concentrating factor for toluene likely arises from liquid's low surface tension and pinning behavior on the platform. Nevertheless, quantitative ultratrace sensing of food toxins is achieved for melamine in water and sudan I in toluene down to 0.1 fmol, with AEFs >10^{11} and >10^{8}, respectively. While this work is the first realization of oleophobic SERS platform, it remains experimentally challenging to realize superomniphobic SERS platform that possesses both superhydrophobic and superoleophobic properties.

Besides the aforementioned superhydrophobic/oleophobic SERS platforms, non-pinning slippery liquid-infused porous surfaces (SLIPS) are also emerging enablers for SERS detection in non-aqueous solvents and biological fluids (Figure 8). In SLIPSERS,[18] nanotextured Teflon membranes are first infiltrated with a perfluorinated liquid that functions as an immiscible lubricant against various aqueous and organic solvents. Subsequent introduction of liquid droplet containing analytes and plasmonic nanoparticles to the membrane surface does not exhibit any solvent pinning. Hence, the droplets evaporate in a constant contact angle mode until complete drying is achieved. This results in the formation of 3D

ensemble structures comprising ~ 2,000 Au nanoparticles/μm^2 interpenetrated with analyte molecules. Besides reaching a detection limit of 1 aM for R6G (50 μL; equivalent to ~30 molecules) in ethanol, SLIPSERS platform also allows quantitative sensing of various dissolved analytes at sub-femtomolar concentrations, including biological species (bovine serum albumin) and environmental contaminants (bis(2-ethyl-hexyl) phthalate). While innovative, the key concerns in this strategy lie in the need to select suitable lubricating liquids that fulfil several criteria, including good adherence within the porous support, immiscibility with sample droplets, sufficiently non-volatile for efficient concentration of analyte/particle and most importantly, does not generate interfering SERS signals. Moreover, this platform only works for liquid-soluble analytes and is unsuitable for the direct enrichment of gaseous and/or volatile chemical species for SERS sensing.

3.4 Using secondary sorbent material for direct concentration of volatile molecules on electromagnetic hotspots

Thus far, our discussion on various analyte concentrating strategies revolves around the capturing and enriching of target molecules in the liquid phase. In contrast to liquid-phase detection, SERS detection of gaseous analytes is inherently more challenging because molecules in the gas phase are intrinsically dilute, exhibit higher mobility, and typically possess minimal affinity toward plasmonic surfaces.[11, 39] Consequently, enormous energy input (such as high pressure and temperature) is required to overcome the unfavorable reduction in entropy to deposit gas/vapor onto SERS substrates. To address this difficulty in gas sensing, metal-organic-frameworks (MOFs) have been integrated with plasmonic nanostructures/nanoparticles to create novel MOF-SERS systems (Figure 9).[11, 39] MOFs are highly porous crystalline structures arising from the extensive coordination network of metal ions and organic linkers, with specific surface areas up to 7000 m^2/g.[40] More importantly, judicious selection of metal ions and organic linkers impart MOFs with tunable 3D sub-nanoscopic pores and a rich abundance of chemical moieties that can be employed for targeted sorption of gas species. In a typical MOF-SERS platform, the MOF component provides a host network for the accumulation of gaseous molecules onto the plasmonic

surfaces via its multifold host-guest chemistry. Such molecular enrichment can generate several orders of magnitude enhancement in SERS signals as compared to bare particles at ambient conditions, thus constituting an attractive strategy to selectively confine and detect small gaseous analytes that usually have poor SERS activity.[39]

Generally, there are two synthetic approaches to form MOF-SERS platforms. In the first approach, MOF is first created followed by the impregnation and reduction of metallic precursors to form plasmonic particles inside the MOF network.[40] However, this method lacks precise control over the size/shape of nanoparticle and interparticle spacing, which could potentially lead to weak and inhomogeneous SERS hotspot distribution within the MOF structure. To overcome such limitation, a second approach is proposed where pre-defined SERS hotspots are first formed via the synthesis and assembly of size-/shape-controlled metallic nanostructures,[11] followed by coating with a layer of MOF. In this review, we focus on the second approach because it can be easily integrated with any hotspot engineering strategies to achieve ultrasensitive and reproducible SERS detection of gas and volatile organic compounds (VOCs).

MOF's gas-enriching ability has allowed MOF-SERS platforms to be successfully utilized in the detection of VOCs. VOCs represent a broad class of molecules with high vapor pressure and low boiling points, which can lead to serious environmental pollution, have detrimental health effects upon prolonged exposure, and can even be used as potential disease biomarkers.[8] However, their detection remains challenging due to their low concentrations, especially at ambient conditions. Integrating ZIF-8 onto gold superparticle (GSP) with 3D engineered hotspots results in a 1.5-fold enhanced sensitivity towards gaseous p-aminothiophenol as compared to bare gold nanoparticles.[8] Moreover, GSP@ZIF-8 also enables quantitative detection of 4-ethylbenzaldehyde, a VOC biomarker for early cancer diagnostics, down to a 10^8 vol/vol level (equivalent to ppb concentration) with high selectivity against other VOCs present in simulated lung cancer breath. On the other hand, Ag film-over-nanospheres (FON)@ZIF-8 array has been demonstrated to detect a library of VOCs with no affinity to Ag,[39] including toluene, benzene (detection limit, 540 ppm), pyridine, nitrobenzene, or 2,6-di-tert-butylpyridine liquid. Specific vibrational fingerprints corresponding to every gaseous analyte can be detected on this platform, thus preventing false

signals and interferences between analytes of similar chemical structures and properties as commonly encountered in conventional commercial gas sensors. However, Ag FON@ZIF-8 array potentially suffers poor SERS activity owing to the use of polycrystalline Ag film with poor Q-factor as the SERS-active surface. More recently, an integration of MOF-based analyte confinement with bottom-up hotspot engineering enables the creation of a 'plasmonic nose',[11] with the capability to detect VOCs down to ppb levels. This strategy first uses Langmuir-Blodgett technique to achieve a densely packed array of crystalline Ag nanocubes with large-area intense electromagnetic field enhancements, followed by the subsequent coating of ZIF-8 to create the plasmonic nose. This plasmonic nose can sense a library of gaseous species including chloroform, naphthalenethiol, toluene, and 4-methylbenzenethiol at the molecular level with ~5-fold better detection sensitivity as compared to similar Ag array without MOF coating.

Another key attribute of using MOF in SERS detection is their ability to selectively enrich target molecules at plasmonic surfaces, effectively filtering out potential interfering molecules from a complex matrix. Molecular selectivity is typically achieved by tuning MOF's pore size in a nanoparticle@MOF composite and imparting these pores with specific chemical functionalities. For instance, a library of small molecules (kinetic diameters <15 Å) such as benzidine, 4-aminothiophenol, diphenylamine, 4,4-bipyridine, and p-phenylenediamine can be selectively detected at ppb-levels using AuNP/MIL-101 composite (MIL denotes Matérial Institut Lavoisier; pore sizes 21.4 Å) via coordination-based host-guest chemistry within its pores (Figure 9a-c).[41] Notably, selective detection of p-phenylenediamine can be attained at 1.3 ng/mL, even from sewage water and river water matrices, which are known to contain multiple molecular contaminants/interferences. This achievement highlights the capability of MOF-SERS substrate as a multi-functional sensing platform that simultaneously provides on-site molecular sieving and SERS detection of small target analytes.

Beyond sensing, the molecular enrichment ability of MOF near plasmonic surfaces also provides an ideal platform to investigate gas-solid interactions, which form the basis for a multitude of heterogeneous catalytic reactions. Dynamic SERS monitoring of CO_2 behaviors within a Ag@ZIF-8 composite under

ambient conditions shows that increasing local gas concentration at the Ag-MOF interface causes CO_2 molecules to transform from linear to bent conformations (Figure 9d-f).[42] Such structural transformation arises from the continuous accumulation of CO_2 molecules into a pseudo high-pressure microenvironment within the interfacial cavities at plasmonic particle-MOF interface. This finding is useful for the design of efficient MOF-SERS gas sensor and holds tremendous promises in the fundamental understanding of heterogeneous solid-gas dynamics even at ambient conditions, which are notably challenging using other characterization techniques.

Integrating porous materials such as MOF with plasmonic nanoparticles effectively synergizes targeted analyte concentrating effects with hotspot engineering for ultrasensitive detection of various gaseous analytes. Nevertheless, there are limitations on these platforms that can be further refined. Analyte confinement at SERS-active surfaces is diffusion-limited because this process requires the diffusion of analyte from the bulk phase to the pores and eventually to the plasmonic surfaces. In MOF-based systems, this limitation is especially pronounced when analyte's size approaches MOF's aperture pore size, and cannot be simply overcome by increasing MOF's aperture size because molecular selectivity will be affected. An effective balance between analyte diffusion and size-selectivity is clearly essential and should be tailored and optimized for each gas-specific application. Moreover, these porous materials could also potentially contribute background SERS interferences during SERS measurement, especially when high laser excitation power is used. It is therefore critical to consider the background SERS spectrum from MOF/porous materials during the substrate optimization to ensure that these background signals do not interfere significantly with the detection of target analytes.

4. Emerging Hybrid SERS Platform for Direct Electromagnetic and/or Chemical Enhancements

To boost SERS sensitivities, secondary functional materials are typically incorporated with conventional metallic nanoparticle-based SERS platforms, including graphene,[20] semiconductors,[12] and piezoelectric polymers.[43] Unlike the materials discussed in section 3, these materials can impart an additional chemical enhancement to complement the strong EM enhancements generated by the metallic

nanoparticles. Consequently, such hybrid SERS platforms can potentially improve the detection limits by 10–10^2-fold as compared to conventional metallic nanoparticle-based SERS platforms,[21] which are especially useful for sensing low analyte concentrations. Furthermore, hybrid SERS platforms integrate the inherent properties of both materials to overcome the limitations of traditional noble metal-only SERS platforms, such as enhanced analyte affinity near plasmonic surfaces, increased stability and higher reproducibility. A notable example is the recent integration of a pi-conjugated organic semiconducting film with a thin Au film to achieve sub-zeptomole methylene blue detection.[44] In the subsequent sections, we focus on three different representative burgeoning materials – graphene, semiconductors and piezoelectric polymers – and categorize them based on the types of synergistic SERS enhancement mechanisms and additional functions that can be conferred to the hybrid ensemble (Table 3). Graphene and semiconductors generate additional chemical enhancements by enabling electronic interactions due to their strong charge transfer capabilities,[12, 20] whereas piezoelectric polymers offer on-demand electric-field-induced enhancements.[43]

4.1 Graphene

Graphene is an atomically thin 2D honeycomb lattice of carbon atoms exhibiting a continuous energy band gap, high surface area, good biocompatibility, superior chemical stability and mechanical strength.[20, 21] With zero bandgap and abundant π -electrons, graphene enhances the Raman scattering of the molecules via a ground-state chemical interaction between the π-electrons and the molecules. Such charge transfer processes enhance electron-phonon coupling and hence induces additional Raman enhancement (Figure 10a).[45] Moreover, graphene can selectively enhance vibrational modes involving π or lone pair-electrons due to stronger π-coupling between the analytes and graphene. These unique attributes of graphene culminate in an additional SERS enhancement of 10–10^2-fold when combining graphene with noble metal nanostructures to form graphene-based hybrid SERS platforms, whereby metallic nanoparticles generally promote SERS via EM enhancement while graphene mainly contributes via additional CHEM enhancement. For example, the addition of graphene oxide to Au nanopopcorn

particles results in >10^2-fold increase in EF from 1.2×10^9 to 3.8×10^{11} and permits detection of HIV DNA on the femto-molar level (Figure 10b).[21]

To design graphene-based hybrid SERS systems, we generally need to consider three key interactions namely (1) graphene and analyte molecules (CHEM), (2) graphene and metal nanoparticles (EM), and (3) metal nanoparticles and analyte (CHEM and EM). For (1), the CHEM enhancement conferred by graphene-analyte interactions largely depends on two factors: the relative position of graphene to the plasmonic nanoparticles and probe molecules, and the oxidation extent of graphene in the hybrid SERS platform. Typically, the CHEM enhancement arises due to π-π stacking and charge transfer between the lone-pairs electrons on oxygen-containing moieties of GO and the aromatic probe molecules. For instance, a single Ag octahedron encapsulated with graphene oxide (GO) flakes (Ag@GO) composite achieves 2-fold higher EF than a Ag octahedron on a GO flake (GO@Ag) composite (9.2×10^5 and 5.4×10^5, respectively).[20] The enhanced SERS performance of Ag@GO arises from the higher surface area GO in contact with the Ag octahedron. Furthermore, the oxidation extent of graphene used in this composite system also affects the SERS enhancements, in which as-synthesized GO affords 35% stronger SERS intensity from the Raman probe (4-methylbenzenethiol) as compared to reduced-GO. In addition, Ag@GO platform exhibits a detection limit of 0.1 nM for aromatic molecules such as R6G, two orders of magnitude lower than that of pure Ag octahedra. This observation emphasizes the importance of integrating plasmonic structures with a secondary material to yield SERS-enhancing synergistic effects not present in the individual component materials.

Aside from pure CHEM, graphene can also improve SERS via a synergistic EM mechanism upon intimate contact with metallic nanostructures. Typically, direct contact between graphene with a metal of higher work function (such as Au) results in an electron flow from graphene to the Au surface through p-doping, contributing to higher EM enhancement from Au. Moreover, it is also possible to achieve additional CHEM enhancement if the HOMO of Au shifts closer to the lowest unoccupied molecular orbital (LUMO) of the chemisorbed molecular probe. For example, a hybrid R6G/AuNP/graphene

platform achieves a 86-fold and 4-fold improvement to SERS signal relative to a R6G/graphene platform and R6G/AuNP platform,[45] respectively. However, we also note that such synergy is highly dependent on the type of metal and its work function with respect to graphene. For example, using Ag of lower work function will result in weak n-doping instead of p-doping of graphene, which will deter the aforementioned synergistic EM/CHEM enhancement.

Another important feature of graphene is that it can suppress fluorescence background of dye molecules by ~10^3-times via Forster resonance energy transfer.[46] Such phenomenon prevents the analyte's vibrational fingerprints from being masked by the broad and intense electronic transition, and leads to improved signal-to-noise ratios. For instance, fluorescence quenching in hybrid systems occurs via additional non-radiative electron transfer from R6G to metallic Ag nanoparticles,[46] enabling a further decrease in the fluorescence of R6G from 50% to 28%.

Compared to previous examples that mostly employ few-layer graphene, a recent graphene-mediated SERS (G-SERS) tape composing of only monolayer graphene with gold/silver nanoislands tightly adhered on its backside has afforded a flat SERS platform (Figure 10c).[47] This G-SERS tape enhances spectral reproducibility and averts broad background peaks originating from photocarbonization of surface carbon adsorbates commonly present in SERS. Additionally, the graphene/metal hybrid's flat surface also provides a more homogeneous molecular orientation for the probe molecules, thus reducing spectral variances that typically arise from heterogeneous molecular configurations on non-atomically flat metallic nanoparticles. However, the most distinct drawback of G-SERS is its intrinsic carbon peaks at ~1580 and 2700 cm^{-1}. These carbon peaks potentially hinder molecular sensing and differentiation of trace analytes because the analytes' SERS features are often overshadowed by graphene's carbon peaks. It is also noteworthy that chemical enhancement brought about by graphene is largely restricted to aromatic compounds that have significant π-π interaction with graphene's π-system, inadvertently limiting the application scope of the graphene/metal hybrid platforms.

4.2 Semiconductors

Semiconductors are a class of materials with composition-dependent band gaps, possessing unique optical, electrical and physical properties that find versatile applications as field-effect transistors, photocatalysts and electrical circuit components.[12, 48, 49] Similar to graphene, semiconductors can also enhance SERS by ~10–10^3-fold through various mechanisms, including surface plasmon, tunable band gap, charge transfer, exciton and molecular resonance. Notably, the ability to tailor the band gap, conduction and valence band edges, and refractive index of semiconductors makes it theoretically possible to tune these properties to match the energy levels for a target molecule for optimal SERS chemical enhancement.

In a typical hybrid semiconductor/metal SERS platform, photoexcited electrons arising from the metal's LSPR flow into the semiconductor's conduction band to promote subsequent semiconductor-to-molecule charge transfer process for CHEM-based SERS enhancement (Figure 11a).[49] The semiconductor nanoparticle acts as a bridge to facilitate electron transfer between the metal and the molecule, because the large energy difference between metal's excited state and molecule's LUMO does not favor direct charge transfer. Such phenomenon has been demonstrated using Au-TiO_2 nanocomposites, whereby SERS intensities of 4-mercaptobenzoic acid (MBA) are enhanced by >3-fold as compared with Au-only and TiO_2-only controls, achieving an EF of 7×10^3.

However, this charge transfer effect is highly dependent on the work function of the metallic nanoparticles, the band gap of the semiconductors used, as well as the overall configuration of the metal/semiconductor/molecule system. For example, in a sandwiched TiO_2/MBA/Ag (semiconductor/molecule/metal) configuration, the lower Ag Fermi level relative to the surface state energy level (E_{ss}) of TiO_2 causes Ag to draw electrons from molecules, and therefore induces additional TiO_2-to-molecule charge transfer (Figure 11b) for stronger SERS enhancement.[50] In contrast, this charge transfer weakens when Au is used for the semiconductor/molecule/metal system due to its lower electronegativity, in turn leading to lower MBA's SERS intensity. Hence, judicious selection of parameters to match the band gap with the electronic structure of target molecules is required to fully exploit the chemical effect of semiconductors.

Recently, employing pre-photoactivated semiconductors with plasmonic nanoparticles results in photo-induced SERS enhancements (PIERS),[12] and gives rise to a >10-fold enhancement as compared to conventional SERS using the semiconductor/metal platform without pre-activation. Pre-irradiating the semiconductor/metal composite with ultraviolet light before analyte deposition generates oxygen vacancy defects (V_o) and results in the formation of a V_o state at an energy level slightly below the semiconductor conduction band edge. The presence of V_o state facilitates electron transfer by allowing the electrons to transit from the V_o state to the conduction band, and eventually to the metal energy levels upon Raman laser irradiation. This charge transfer process also shifts the metal's Fermi level to a broad distribution of more negative values, extending the resonance overlap between the metal's Fermi level and the analyte's molecular orbitals. This in turn increases the charge transfer transition probabilities, which are independent on the nature of the molecule and can be universally applied over a wide variety of analytes to improve detection sensitivity, especially for those with small Raman cross-sections. For example, Au nanoparticles deposited on a rutile TiO_2 surface enable trinitrotoluene detection down to 10^{-8} M,[12] which is unachievable previously because additional chemical enhancement from charge transfer is restricted due to energy mismatch between metal and analyte.

In addition to charge transfer, one-dimensional (1D) high refractive index semiconductors can also interact with metals to enhance the local EM field at the heterojunction for additional SERS enhancement. For instance, direct contact between ZnO semiconductor and a metal allows the electronic states of the semiconductor to interact with the dielectric-confined EM modes of the metal.[48] This interaction results in charge transfer from metal to semiconductor and prevents the recombination of electron-hole pairs. Consequently, the exciton-plasmon interaction localizes the electric field at the gap between the two materials and contributes to a large EM field enhancement. This phenomenon is again observed in hybrid SERS platform formed by depositing ZnO nanofibers on Ag foil surface, whereby p-aminothiophenol is detected down to 10^{-12} M and with a EF of 10^8 and >30-fold improvement compared to Ag-only platform.

Semiconductors also exhibit unique photocatalytic and self-cleaning capabilities, which can be integrated with plasmonic nanoparticles to extend SERS to practical applications and mechanistic

investigations. For example, in-situ SERS measurements using ZnO/metal system reveals enhanced photocatalytic degradation of organic pollutants upon UV irradiation owing to improved charge separation of this hybrid platform.[48] Photocatalytic semiconductors brings about additional self-cleaning ability to the hybrid substrates, allowing them to be recycled by subjecting the hybrid SERS platform to UV light for near-complete analyte degradation.[49] Such self-cleaning property is unique to photocatalytic semiconductors and can extend SERS toward more practical and economical applications by offering additional stability and recyclability. Despite the diversity and versatility of semiconductors, we note a lack of research on designing semiconductor/metal platforms for selective molecule detection. Another potential drawback is that charge transfer creates a Raman shift of analyte's intrinsic vibrational fingerprint, consequently leading to peak broadening and increased difficulty in their accurate interpretation.

4.3 Piezoelectric polymers

Piezoelectric materials convert mechanical energy to electrical energy upon structural deformation.[43] When coupled with a metal, deforming the piezoelectric polymer creates a negative potential whereby electrons are injected into the metallic component to increase the local electric field at the hotspot, and thereby enhances SERS intensities. This enhancement effect is similar to that of conventional electrochemical-SERS (EC-SERS) platforms,[43] which utilizes electric-field to enhance adsorption at negative potentials and gives rise to excess electrons in the conductance band of metal to yield stronger LSPR/EM field (analogous to lightning-rod effect of electric field). More importantly, piezoelectric-based hybrid SERS system offers a competitive edge over conventional EC-SERS because it does not need bulky apparatus (such as potentiostat) and instead relies on simple mechanical stimulation to achieve on-demand electric-field enhancements. To this end, a self-energizing SERS substrate has been demonstrated by combining Ag nanowires with a polymeric composite piezoelectric film comprising poly(vinylidene fluoride-co-hexafluoropropylene (PVDF-HFP) and reduced-GO (Figure 12).[43] A negative electric potential of up to 2.6 V is generated on the substrate surface upon deformation, which

enhances local electric field by >3-fold (using FDTD simulations) and increases SERS readout by 10-fold. While chemical enhancement is also likely present due to the slight shifts in peaks as compared to the discharged states, the actual contribution of chemical enhancement has not yet been elucidated. Therefore, piezoelectric polymer breaks away from the typical secondary materials that contributes mainly via chemical enhancement. Despite the EM-based enhancements, the actual improvement to Raman intensity is relatively low and there is certainly room for improvement in the system by optimizing each component of the hybrid system to achieve stronger SERS readouts.

Current hybrid systems typically utilize materials to introduce additional chemical enhancements and boost overall SERS sensitivities. However, a common limitation for such hybrid SERS materials is that it requires chemical or physical binding to achieve optimal chemical enhancement via charge transfer, which again restricts the choice of analyte to thiolated or aromatic analytes. There are also limited reports on the use of hybrid systems to improve SERS via EM, which theoretically allow far drastic advancements in addition to charge transfer mechanism.

5. Conclusions & Outlook

In this tutorial review, we have covered the recent development of SERS platforms enabled by hotspot engineering, as well as emerging strategies involving analyte manipulation and hybrid SERS platform designs. Progress in top-down and bottom-up nanofabrication approaches has given rise to the ability for precision engineering of plasmonic nanostructures into multi-dimensional designer hotspots with stronger field enhancement and unique structure-to-plasmon properties. Beyond traditional hotspot engineering, our review demonstrates how analyte manipulation strategies play a central role to further improve SERS platforms for better sensitivity and broader analytical applications. These strategies primarily work by directing and confining analytes into electromagnetic hotspots where field enhancement and corresponding SERS intensities will be the strongest. Four different analyte manipulation strategies are identified according to their individual underlying principles, which notably exploit (1) molecular coupling reactions, (2) surface-grafted analyte-capturing agents, (3) surface non-

wetting phenomena and (4) molecule sorbent layers. We also emphasize the facile integration of these analyte manipulation strategies with well-designed electromagnetic hotspots to fully exploit the multiplicative benefits imparted by both distinct-yet-complementary SERS enhancing mechanisms. Furthermore, we provide an overview on the growing efforts to couple SERS platforms with other functional materials to directly modulate and improve the ensemble's electromagnetic and chemical properties for better SERS performance. Notable examples of these materials include 2D materials and stimuli-responsive electronic materials.

While promising, these approaches are still in their infancy and we have identified four major challenges to be addressed. First, it remains a formidable challenge in hotspot engineering to design efficient 3D plasmonic architectures for effective electromagnetic field utilization along z-plane (plane along laser path) without sacrificing light accessibility. Moreover, the fabrication of large-area and homogeneous hotspot necessary for uniform SERS read-out is non-trivial and requires further advances in both top-down and/or bottom-up nanofabrication approaches. Future work in these topics could be directed to the use of hollow or open-structured particles as the building blocks in the construction of 3D SERS platforms. These particles exhibit good SERS activity owing to their high specific areas along with the presence of strong field confinement at their vertices/edges. More importantly, hollow frame structures allow better light penetration compared to their solid counterparts. This attribute can be further leveraged to realize 3D plasmonic scaffolds with efficient light accessibility and dense hotspot distributions. Achieving efficient 3D plasmonic hotspots is necessary to generate intense field enhancement and even uncover novel multidimensional plasmonic phenomena that can be exploited to boost SERS performance.

Second, ultratrace detection of oil-soluble (bio)molecules and liquid analytes also remains difficult, especially for organic liquids with low surface tension because they spread readily and dilute analytes over SERS substrate. Overcoming this hurdle is crucial because these analytes are ubiquitous in diverse real-life applications, such as water pollution management, food safety, and chemical manufacturing. We hypothesize that the realization of superoleophobic SERS platform could potentially address this limitation by concentrating oil-soluble/liquid analyte molecules directly onto the electromagnetic hotspots,

similar to the working mechanism of its superhydrophobic counterpart. This strategy could also be extended to superomniphobic platforms – exhibiting both superhydrophobicity and superoleophobicity – to enable the universal and ultratrace SERS detection of both aqueous- and oil-soluble analytes in a single substrate. To date, superoleophobic and superomniphobic SERS platforms have not been realized and possibly requires the strategic design of re-entrant structures besides creating surface roughness and modifying surface chemistry.

Third, moving towards detection in real-world sample, it is also important to employ statistical tools (such as principal component analysis) to accurately identify/differentiate vibrational signatures of target analytes from other molecular interferences. This is especially crucial in a highly complex biological matrix with a myriad (bio)molecules that is difficult to decipher the individual molecular fingerprints. Moreover, we could also employ a combinatorial SERS approach to determine a sophisticated molecular structure by identifying the analyte's key functional groups through their complementary interactions with known surface-grafted molecular probes. Such systematic and comprehensive SERS evaluations boost the level of confidence in molecular recognition by increasing the number of "identification points" on the analyte. This method is particularly useful to elucidate large molecular structures where it is near impossible to directly decipher their highly complex vibrational fingerprints.

Fourth, current studies on hybrid SERS platforms mainly focus on identifying the mechanism of synergistic effects arising from the interaction between plasmonic nanostructures and secondary functional materials, usually at the single particle level. There is a lack of demonstration on the large-scale fabrication of these hybrid SERS ensembles with high batch-to-batch reproducibility, as well as a lack of report on the formation of SERS hybrid platforms using precisely engineered 2D/3D hotspots. Achieving facile fabrication of hybrid SERS platforms and their combination with well-designed multi-dimensional hotspots are crucial and the first step towards practical SERS sensing applications. Moreover, we anticipate future integration of hybrid SERS platform with analyte manipulation techniques. Such integration offers a multitude of functionalities, directly impacting EM/CHEM enhancement mechanisms and plasmonic surface-analyte interactions to achieve efficient and ultrasensitive SERS read-out.

All in all, both analyte manipulation and the incorporation of SERS platform with other functional materials offer immensely attractive strategies to potentially overcome the limitations in SERS sensing, which cannot be addressed by traditional hotspot engineering alone. These strategies lead to a paradigm shift beyond hotspot engineering, which is critical to ensure continuous improvement of SERS platforms in term of their sensitivity and practicality. By converging the research advances and advantages of individual scientific/engineering disciplines, we can certainly anticipate thriving research in such multi-faceted approaches to lead to a rapid breakthrough in the design of next-generation hybrid SERS platforms. Realizing multi-functional SERS devices is important to open new opportunities in fundamental molecular-level studies as well as real-world analytical applications in diverse fields including synthetic chemistry, disease recognition as well as environmental and life conservations.

Acknowledgements

X.Y.L. thanks the financial supports from Singapore Ministry of Education, Tier 1 (RG21/16) and Tier 2 (MOE2016-T2-1-043) grants. C.L.L. acknowledges the A*STAR Graduate Scholarship from A*STAR, Singapore. C.S.L.K. and G.C.P-Q acknowledge support from Nanyang Presidential Graduate Scholarship from Nanyang Technological University. Q.A. thanks the funding support from NSFC (21303169, 21673209, 51572246), the Fundamental Research Funds for the Central Universities (2652015295), Beijing Nova Program (Z141103001814064).

References

1. M. F. Cardinal, E. Vander Ende, R. A. Hackler, M. O. McAnally, P. C. Stair, G. C. Schatz, R. P. Van Duyne, Expanding applications of SERS through versatile nanomaterials engineering, *Chem. Soc. Rev.,* 2017, **46**, 3886-3903.
2. S.-Y. Ding, E.-M. You, Z.-Q. Tian, M. Moskovits, Electromagnetic theories of surface-enhanced Raman spectroscopy, *Chem. Soc. Rev.,* 2017, **46**, 4042-4076.
3. G. C. Phan-Quang, H. K. Lee, I. Y. Phang, X. Y. Ling, Plasmonic colloidosomes as three-dimensional SERS platforms with enhanced surface area for multiphase sub-microliter toxin sensing, *Angew. Chem. Int. Ed.,* 2015, **54**, 9691-9695.
4. M. Jahn, S. Patze, I. J. Hidi, R. Knipper, A. I. Radu, A. Mühlig, S. Yüksel, V. Peksa, K. Weber, T. Mayerhöfer, D. Cialla-May, J. Popp, Plasmonic nanostructures for surface enhanced spectroscopic methods, *Analyst,* 2016, **141**, 756-793.

5. S.-Y. Ding, J. Yi, J.-F. Li, B. Ren, D.-Y. Wu, R. Panneerselvam, Z.-Q. Tian, Nanostructure-based plasmon-enhanced Raman spectroscopy for surface analysis of materials, *Nature Reviews Materials,* 2016, **1**, 16021.
6. G. C. Phan-Quang, H. K. Lee, X. Y. Ling, Isolating reactions at the picoliter scale: Parallel control of reaction kinetics at the liquid–liquid interface, *Angew. Chem. Int. Ed.,* 2016, **55**, 8304-8308.
7. X. Han, H. K. Lee, Y. H. Lee, W. Hao, Y. Liu, I. Y. Phang, S. Li, X. Y. Ling, Identifying enclosed chemical reaction and dynamics at the molecular level using shell-isolated miniaturized plasmonic liquid marble, *J. Phys. Chem. Lett.,* 2016, **7**, 1501-1506.
8. X. Qiao, B. Su, C. Liu, Q. Song, D. Luo, G. Mo, T. Wang, Selective surface enhanced Raman scattering for quantitative detection of lung cancer biomarkers in superparticle@MOF structure, *Adv. Mater.,* 2018, **30**, 1702275.
9. X. X. Han, P. Pienpinijtham, B. Zhao, Y. Ozaki, Coupling reaction-based ultrasensitive detection of phenolic estrogens using surface-enhanced resonance Raman scattering, *Anal. Chem.,* 2011, **83**, 8582-8588.
10. X. Li, H. K. Lee, I. Y. Phang, C. K. Lee, X. Y. Ling, Superhydrophobic-oleophobic Ag nanowire platform: An analyte-concentrating and quantitative aqueous and organic toxin surface-enhanced Raman scattering sensor, *Anal. Chem.,* 2014, **86**, 10437-10444.
11. C. S. L. Koh, H. K. Lee, X. Han, H. Y. F. Sim, X. Y. Ling, Plasmonic nose: integrating the MOF-enabled molecular preconcentration effect with a plasmonic array for recognition of molecular-level volatile organic compounds, *Chem. Commun.,* 2018, **54**, 2546-2549.
12. S. Ben-Jaber, W. J. Peveler, R. Quesada-Cabrera, E. Cortés, C. Sotelo-Vazquez, N. Abdul-Karim, S. A. Maier, I. P. Parkin, Photo-induced enhanced Raman spectroscopy for universal ultra-trace detection of explosives, pollutants and biomolecules, *Nat. Commun.,* 2016, **7**, 12189.
13. S. Y. Lee, S.-H. Kim, M. P. Kim, H. C. Jeon, H. Kang, H. J. Kim, B. J. Kim, S.-M. Yang, Freestanding and arrayed nanoporous microcylinders for highly active 3D SERS substrate, *Chem. Mater.,* 2013, **25**, 2421-2426.
14. Y. H. Lee, C. L. Lay, W. Shi, H. K. Lee, Y. Yang, S. Li, X. Y. Ling, Creating two self-assembly micro-environments to achieve supercrystals with dual structures using polyhedral nanoparticles, *Nat. Commun.,* 2018, **9**, 2769.
15. V. Ranc, Z. Markova, M. Hajduch, R. Prucek, L. Kvitek, J. Kaslik, K. Safarova, R. Zboril, Magnetically assisted surface-enhanced Raman scattering selective determination of dopamine in an artificial cerebrospinal fluid and a mouse striatum using Fe_3O_4/Ag nanocomposite, *Anal. Chem.,* 2014, **86**, 2939-2946.
16. D. Tsoutsi, J. M. Montenegro, F. Dommershausen, U. Koert, L. M. Liz-Marzán, W. J. Parak, R. A. Alvarez-Puebla, Quantitative surface-enhanced Raman scattering ultradetection of atomic inorganic ions: The case of chloride, *ACS Nano,* 2011, **5**, 7539-7546.
17. F. De Angelis, F. Gentile, F. Mecarini, G. Das, M. Moretti, P. Candeloro, M. L. Coluccio, G. Cojoc, A. Accardo, C. Liberale, R. P. Zaccaria, G. Perozziello, L. Tirinato, A. Toma, G. Cuda, R. Cingolani, E. Di Fabrizio, Breaking the diffusion limit with super-hydrophobic delivery of molecules to plasmonic nanofocusing SERS structures, *Nat. Photonics,* 2011, **5**, 682.
18. S. Yang, X. Dai, B. B. Stogin, T.-S. Wong, Ultrasensitive surface-enhanced Raman scattering detection in common fluids, *Proc. Natl. Acad. Sci. U.S.A.,* 2016, **113**, 268-273.
19. X. Han, C. S. L. Koh, H. K. Lee, W. S. Chew, X. Y. Ling, Microchemical plant in a liquid droplet: Plasmonic liquid marble for sequential reactions and attomole detection of toxin at microliter scale, *ACS Appl. Mater. Interfaces,* 2017, **9**, 39635-39640.
20. W. Fan, Y. H. Lee, S. Pedireddy, Q. Zhang, T. Liu, X. Y. Ling, Graphene oxide and shape-controlled silver nanoparticle hybrids for ultrasensitive single-particle surface-enhanced Raman scattering (SERS) sensing, *Nanoscale,* 2014, **6**, 4843-4851.
21. Z. Fan, R. Kanchanapally, P. C. Ray, Hybrid graphene oxide based ultrasensitive SERS probe for label-free biosensing, *J. Phys. Chem. Lett.,* 2013, **4**, 3813-3818.
22. K. Kim, H. S. Han, I. Choi, C. Lee, S. Hong, S.-H. Suh, L. P. Lee, T. Kang, Interfacial liquid-state surface-enhanced Raman spectroscopy, *Nat. Commun.,* 2013, **4**, 2182.
23. M. S. Goh, Y. H. Lee, S. Pedireddy, I. Y. Phang, W. W. Tjiu, J. M. R. Tan, X. Y. Ling, A chemical route to increase hot spots on silver nanowires for surface-enhanced Raman spectroscopy application, *Langmuir,* 2012, **28**, 14441-14449.

24. S. Tian, O. Neumann, M. J. McClain, X. Yang, L. Zhou, C. Zhang, P. Nordlander, N. J. Halas, Aluminum nanocrystals: A sustainable substrate for quantitative SERS-based DNA detection, *Nano Lett.,* 2017, **17**, 5071-5077.
25. Y. Liu, S. Pedireddy, Y. H. Lee, R. S. Hegde, W. W. Tjiu, Y. Cui, X. Y. Ling, Precision synthesis: Designing hot spots over hot spots via selective gold deposition on silver octahedra edges, *Small,* 2014, **10**, 4940-4950.
26. Y. H. Lee, W. Shi, H. K. Lee, R. Jiang, I. Y. Phang, Y. Cui, L. Isa, Y. Yang, J. Wang, S. Li, X. Y. Ling, Nanoscale surface chemistry directs the tunable assembly of silver octahedra into three two-dimensional plasmonic superlattices, *Nat. Commun.,* 2015, **6**, 6990.
27. Y. Yang, Y. H. Lee, I. Y. Phang, R. Jiang, H. Y. F. Sim, J. Wang, X. Y. Ling, A chemical approach to break the planar configuration of Ag nanocubes into tunable two-dimensional metasurfaces, *Nano Lett.,* 2016, **16**, 3872-3878.
28. J. Henzie, S. C. Andrews, X. Y. Ling, Z. Li, P. Yang, Oriented assembly of polyhedral plasmonic nanoparticle clusters, *Proc. Natl. Acad. Sci. U.S.A.,* 2013, **110**, 6640-6645.
29. M. R. Lee, H. K. Lee, Y. Yang, C. S. L. Koh, C. L. Lay, Y. H. Lee, I. Y. Phang, X. Y. Ling, Direct metal writing and precise positioning of gold nanoparticles within microfluidic channels for SERS sensing of gaseous analytes, *ACS Appl. Mater. Interfaces,* 2017, **9**, 39584-39593.
30. M. Chen, I. Y. Phang, M. R. Lee, J. K. W. Yang, X. Y. Ling, Layer-by-layer assembly of Ag nanowires into 3D woodpile-like structures to achieve high density "hot spots" for surface-enhanced Raman scattering, *Langmuir,* 2013, **29**, 7061-7069.
31. T. Udayabhaskararao, T. Altantzis, L. Houben, M. Coronado-Puchau, J. Langer, R. Popovitz-Biro, L. M. Liz-Marzán, L. Vuković, P. Král, S. Bals, R. Klajn, Tunable porous nanoallotropes prepared by post-assembly etching of binary nanoparticle superlattices, *Science,* 2017, **358**, 514-518.
32. Q. Zhang, Y. H. Lee, I. Y. Phang, C. K. Lee, X. Y. Ling, Hierarchical 3D SERS substrates fabricated by integrating photolithographic microstructures and self-assembly of silver nanoparticles, *Small,* 2014, **10**, 2703-2711.
33. F. J. M. Hoeben, P. Jonkheijm, E. W. Meijer, A. P. H. J. Schenning, About supramolecular assemblies of π-conjugated systems, *Chem. Rev.,* 2005, **105**, 1491-1546.
34. Q. Zhao, G. Liu, H. Zhang, F. Zhou, Y. Li, W. Cai, SERS-based ultrasensitive detection of organophosphorus nerve agents via substrate's surface modification, *J. Hazard. Mater.,* 2017, **324**, 194-202.
35. A. Balzerova, A. Fargasova, Z. Markova, V. Ranc, R. Zboril, Magnetically-assisted surface enhanced Raman spectroscopy (MA-SERS) for label-free determination of human Immunoglobulin G (IgG) in blood ssing Fe_3O_4@Ag nanocomposite, *Anal. Chem.,* 2014, **86**, 11107-11114.
36. Y. Cao, D.-W. Li, L.-J. Zhao, X.-Y. Liu, X.-M. Cao, Y.-T. Long, Highly selective detection of carbon monoxide in living cells by palladacycle carbonylation-based surface enhanced Raman spectroscopy nanosensors, *Anal. Chem.,* 2015, **87**, 9696-9701.
37. H. K. Lee, Y. H. Lee, Q. Zhang, I. Y. Phang, J. M. R. Tan, Y. Cui, X. Y. Ling, Superhydrophobic surface-enhanced Raman scattering platform fabricated by assembly of Ag nanocubes for trace molecular sensing, *ACS Appl. Mater. Interfaces,* 2013, **5**, 11409-11418.
38. J.-A. Huang, Y.-L. Zhang, Y. Zhao, X.-L. Zhang, M.-L. Sun, W. Zhang, Superhydrophobic SERS chip based on a Ag coated natural taro-leaf, *Nanoscale,* 2016, **8**, 11487-11493.
39. L. E. Kreno, N. G. Greeneltch, O. K. Farha, J. T. Hupp, R. P. Van Duyne, SERS of molecules that do not adsorb on Ag surfaces: a metal–organic framework-based functionalization strategy, *Analyst,* 2014, **139**, 4073-4080.
40. C. Rösler, R. A. Fischer, Metal–organic frameworks as hosts for nanoparticles, *CrystEngComm,* 2015, **17**, 199-217.
41. Y. Hu, J. Liao, D. Wang, G. Li, Fabrication of gold nanoparticle-embedded metal–organic framework for highly sensitive surface-enhanced Raman scattering detection, *Anal. Chem.,* 2014, **86**, 3955-3963.
42. H. K. Lee, Y. H. Lee, J. V. Morabito, Y. Liu, C. S. L. Koh, I. Y. Phang, S. Pedireddy, X. Han, L.-Y. Chou, C.-K. Tsung, X. Y. Ling, Driving CO2 to a Quasi-Condensed Phase at the Interface between a Nanoparticle Surface and a Metal–Organic Framework at 1 bar and 298 K, *J. Am. Chem. Soc.,* 2017, **139**, 11513-11518.

43. H. Li, H. Dai, Y. Zhang, W. Tong, H. Gao, Q. An, Surface-enhanced Raman spectra promoted by a finger press in an all-solid-state flexible energy conversion and storage film, *Angew. Chem. Int. Ed.,* 2017, **56**, 2649-2654.
44. M. Yilmaz, E. Babur, M. Ozdemir, R. L. Gieseking, Y. Dede, U. Tamer, G. C. Schatz, A. Facchetti, H. Usta, G. Demirel, Nanostructured organic semiconductor films for molecular detection with surface-enhanced Raman spectroscopy, *Nat. Mater.,* 2017, **16**, 918.
45. X.-k. Kong, Q.-w. Chen, Z.-y. Sun, Enhanced SERS of the complex substrate using Au supported on graphene with pyridine and R6G as the probe molecules, *Chem. Phys. Lett.,* 2013, **564**, 54-59.
46. Fluorescence quenching due to sliver nanoparticles covered by graphene and hydrogen-terminated graphene, *Appl. Phys. Lett.,* 2013, **102**, 053113.
47. W. Xu, X. Ling, J. Xiao, M. S. Dresselhaus, J. Kong, H. Xu, Z. Liu, J. Zhang, Surface enhanced Raman spectroscopy on a flat graphene surface, *Proc. Natl. Acad. Sci. U.S.A.,* 2012, **109**, 9281-9286.
48. W. Song, W. Ji, S. Vantasin, I. Tanabe, B. Zhao, Y. Ozaki, Fabrication of a highly sensitive surface-enhanced Raman scattering substrate for monitoring the catalytic degradation of organic pollutants, *J. Mater. Chem. A,* 2015, **3**, 13556-13562.
49. X. Jiang, X. Sun, D. Yin, X. Li, M. Yang, X. Han, L. Yang, B. Zhao, Recyclable Au–TiO_2 nanocomposite SERS-active substrates contributed by synergistic charge-transfer effect, *Phys. Chem. Chem. Phys.,* 2017, **19**, 11212-11219.
50. X. Jiang, X. Li, X. Jia, G. Li, X. Wang, G. Wang, Z. Li, L. Yang, B. Zhao, Surface-enhanced Raman scattering from synergistic contribution of metal and semiconductor in TiO_2/MBA/Ag(Au) and Ag(Au)/MBA/TiO_2 assemblies, *J. Phys. Chem. C,* 2012, **116**, 14650-14655.

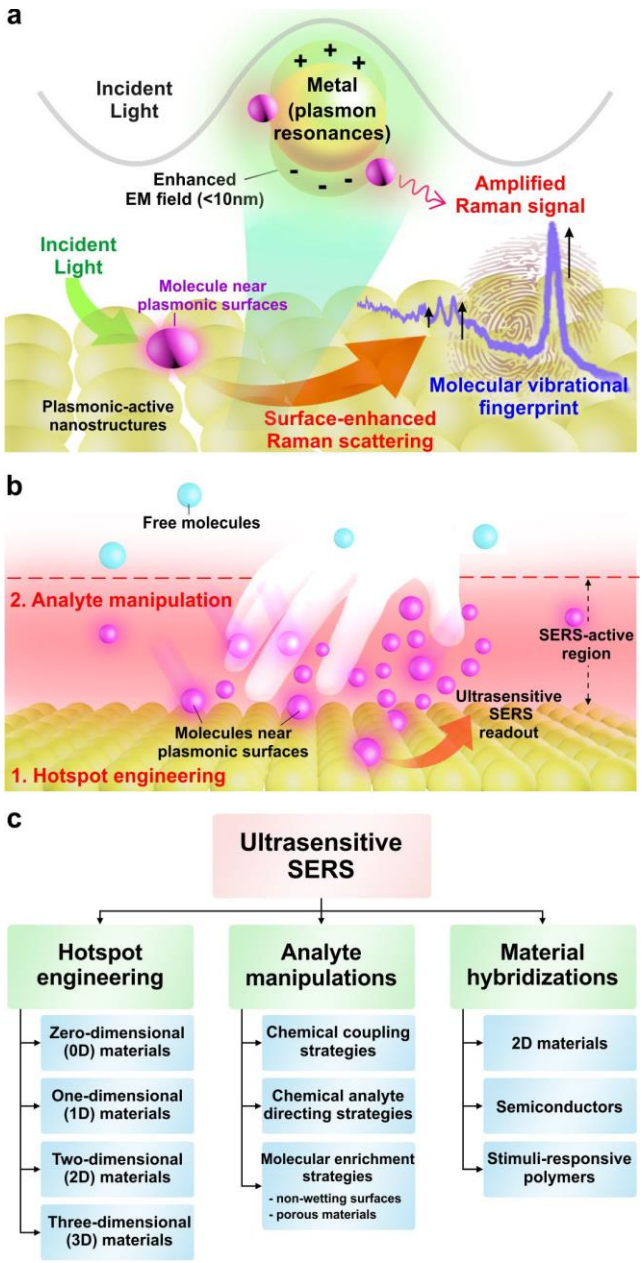

Figure 1: Surface-enhanced Raman scattering (SERS). (a) Scheme depicting the use of noble metal nanostructures to support localized surface plasmon resonances (LSPRs) for SERS enhancement. (b) A two-pronged approach to achieve ultrasensitive SERS readout by integrating analyte manipulation techniques with hotspot engineering. (c) Research roadmap highlighting the importance of hotspot engineering, analyte manipulation and material hybridizations to achieve ultrasensitive SERS.

Table 1: Current progress in electromagnetic hotspot engineering for SERS applications.

SERS platform ^ Plasmonic building block	**Approach**	**Analyte(s)**	**Analyte medium**	**Limit of detection (Limit of quantification)**	**Enhancement factor (EF)/ Analytical enhancement factor (AEF)**	**Comments**	**Ref**
Hotspot engineering (0D - 3D)							
Selective edge gold-deposited silver octahedra (SEGSO) ^ Ag octahedra	0D	4-methylbenzenethiol	ethanol	N.A.	1.1×10^5 * single particle level	15-fold and 10-fold stronger field and EF than bare Ag octahedra	25
Etched Ag nanowire ^ Ag nanowire	1D	4-methylbenzenethiol	ethanol	N.A.	6.4×10^4 * single particle level	SERS activity across entire etched Ag nanowire; in contrast, as-synthesized Ag nanowire only shows SERS activity at both ends	23
2D square-lattice plasmonic metacrystal ^ Ag octahedron	2D	4-methylbenzenethiol	ethanol	N.A.	9.9×10^4	7.5-fold higher than ordered and denser hexagonal arrays	26
Vertically-aligned Au nanorods (GNR) assembled at liquid-liquid interface ^ Au nanorod	2D	rhodamine 6G (R6G) 1-10-diethyl-2-20-cyanine iodide (DCI)	aqueous aqueous	R6G: 10^{-9} M (10^{-9} M) DCI: 10^{-8} M	R6G: 10^6 * AEF	10^4-fold better than random-oriented GNR system	22
Nanoporous microcylinder decorated with Au nanoparticles ^ Au nanoparticle	3D	benzenethiol	ethanol	N.A.	6.5×10^4	10-fold better than that using dense microcylinder	13
Photolithographically-fabricated prism decorated with a compact monolayer of Ag nanocube ^ Ag nanocube	3D	4-methylbenzenethiol	ethanol	N.A.	3.4×10^6	1.2-fold better than 2D SERS platform	32
Plasmonic colloidosome ^ Ag nanocube	3D	methylene blue (MB) rhodamine 6G (R6G) malachite green (MG) coumarin dimethyl yellow (DY)	aqueous aqueous aqueous decane decane	MB: 10^{-9} M (10^{-9} M) R6G: 10^{-9} M (10^{-9} M) MG: 10^{-7} M (10^{-7} M) coumarin: 10^{-9} M (10^{-9} M) DY: 10^{-7} M (10^{-7} M)	MB: 8×10^6 R6G: 2×10^6 MG: 10^5 coumarin: 4.7×10^7 DY: 10^5 * AEF	N.A.	3

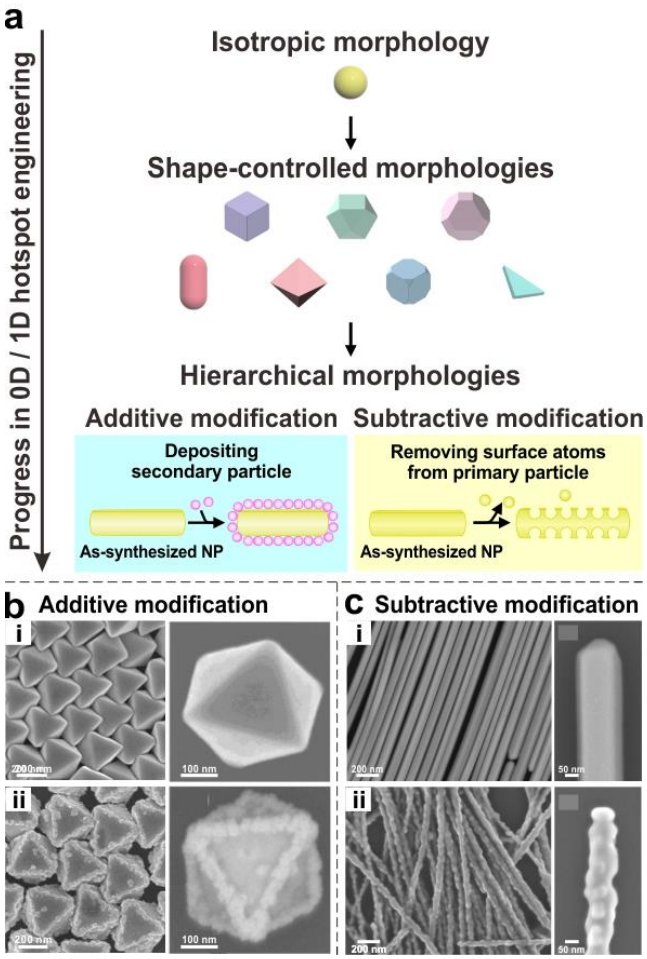

Figure 2. Emerging strategies for 0D/1D hotspot engineering. (a) Overview of the progress in 0D/1D hotspot engineering. (b) Additive post-synthetic modification. (i, ii) SEM images of as-synthesized Ag octahedron and selective edge Au-deposited Ag octahedral (SEGSO), respectively. (c) Subtractive post-synthetic modification. (i, ii) SEM images of as-synthesized Ag nanowires and etched Ag nanowires, respectively. Reprinted and adapted with permission from (b) ref 25 and (c) ref 23. Copyright 2014 John Wiley & Sons, Ltd. Copyright 2012 American Chemical Society.

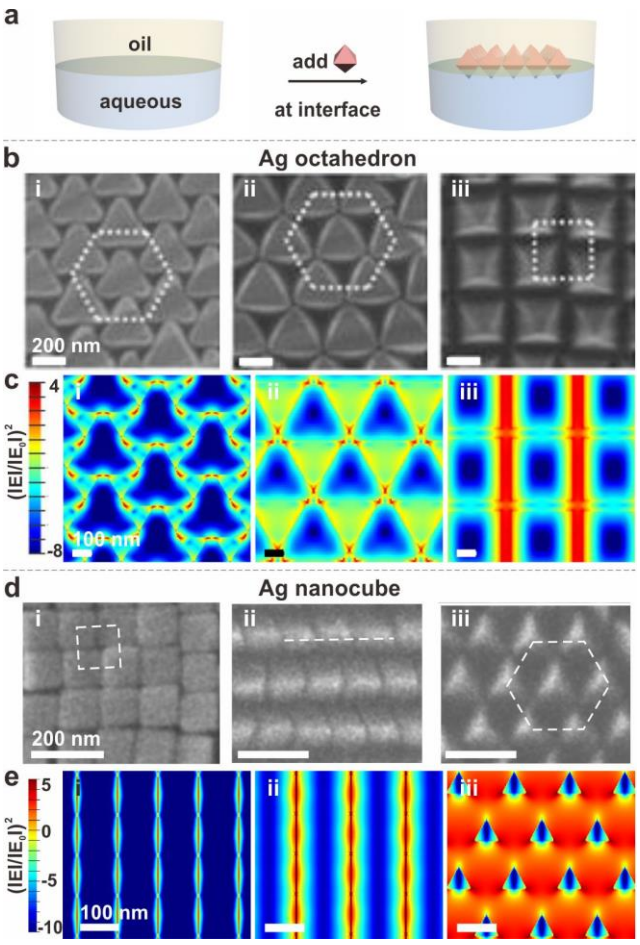

Figure 3. Two-dimensional hotspot engineering. (a) Employing nanoscale surface chemistry to tune two-dimensional metacrystal structures of plasmonic nanoparticles at the oil/water interface. (b) Increasing surface hydrophobicity changes the metacrystal structure from (i) hexagonal close-packed to (ii) open hexagonal and finally to (iii) open square lattices when using Ag octahedron as building blocks. (c) Corresponding electric field distributions of various Ag octahedra-based metacrystals at 532 nm. (d) SEM images and (e) corresponding electric field distributions of Ag nanocube-based metacrystals adopting (i) square close-packed configuration, (ii) tilted nanocube string-like configuration and (iii) standing nanocube configuration. Reprinted and adapted with permission from (a-c) ref 26 and (d, e) ref 27. Copyright 2015 Nature Publishing Group. Copyright 2016 American Chemical Society.

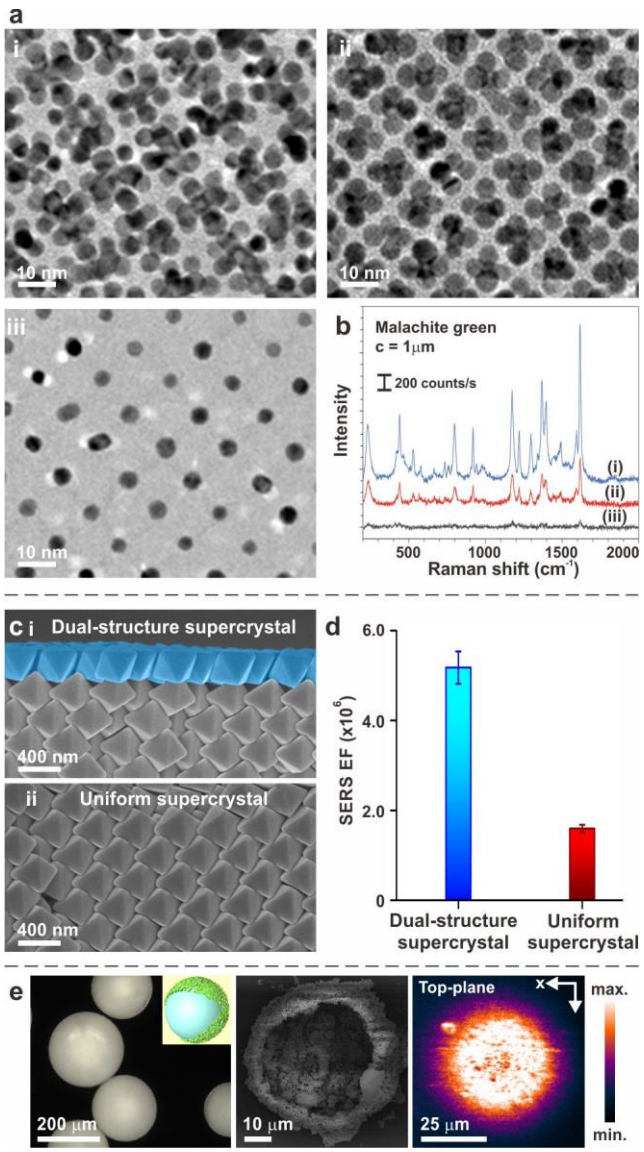

Figure 4. Organizing nanoparticles into three-dimensional SERS-active superstructures. (a) TEM images and (b) corresponding SERS spectra recorded from three different non-close-packed nanoparticle arrays. (i) vac_1Au_1, (ii) vac_1Au_5 and (iii) vac_1Au_{11}, where *vac* denotes vacancy and the subscripted numbers indicate their respective ratio. (c) SEM images of (i) a dual-structure supercrystal and a (ii) uniform supercrystal. (d) Comparison of SERS EF of the corresponding supercrystals in (c). (e) Plasmonic colloidosomes constructed using Ag nanocubes as building blocks. Left, middle and right columns correspond to the optical microscopic image, SEM image and SERS image of plasmonic colloidosome. Reprinted and adapted with permission from (a, b) ref 31, (c, d) ref 14 and (e) ref 3. Copyright 2017 The American Association for the Advancement of Science. Copyright 2018 Nature Publishing Group. Copyright 2015 John Wiley & Sons, Ltd.

Table 2: Design and application of SERS platforms beyond hotspot engineering – Emerging strategies in analyte manipulations.

SERS platform ^ Plasmonic building block	Approach	Analyte(s)	Analyte medium	Limit of detection (Limit of quantification)	Enhancement factor (EF)/ Analytical enhancement factor (AEF)	Comments	Ref
Analyte manipulations							
i. Enlarging molecular Raman cross-sections using chemical coupling approaches							
Plasmonic liquid marble (PLM) ^ Ag nanocube	azo coupling	bisphenol A (BPA) methylene blue (MB)	aqueous aqueous	BPA: 5×10^{-12} M (5×10^{-11} M) MB: 1×10^{-9} M	MB: 4.5×10^{8} *AEF	no bisphenol A's SERS bands detected in the absence of azo coupling	19
Colloidal solution ^ Ag nanoparticle	azo coupling	estrone bisphenol A (BPA)	aqueous	estrone: 3.7×10^{-10} M BPA: 4.4×10^{-10} M	N.A.	no estrogen's SERS bands detected in the absence of azo coupling	9
ii. Chemical analyte directing strategies							
Au-coated Si nanocone array with surface-grafted 2-aminoethanethiol ^ sputtered Au	direct detection	methanephosphonic acid (MPA)	ethanol	10^{-8} M (10^{-8} M)	N.A.	no MPA's SERS bands detected in absence of surface-grafted capturing moiety	34
Fe_3O_4/Ag nanocomposite modified with iron nitriloacetic acid ^ Fe_3O_4/Ag nanoparticle	direct detection (Magnetically-assisted)	dopamine	aqueous artificial cerebrospinal fluid	5×10^{-15} M (6.9×10^{-15} M)	N.A.	N.A.	15
Palladacycle-grafted Au nanoparticles ^ Au nanoparticle	indirect detection	carbon monoxide (CO) (using CO releasing molecule; CORM)	gas (in PBS solution or cell)	3.4×10^{-7} M (5×10^{-7} M; in PBS solution) 5×10^{-7} M (in cell)	N.A.	N.A.	36
SiO_2@Au@Ag grafted with 2-(2-(6-methoxyquinoliniumchloride)ethoxy)-ethanamine-hydrochloride ^ SiO_2@Au@Ag nanocomposite	indirect detection	Cl^-	aqueous	10^{-12} M (10^{-12} M)	N.A.	Cl^- ions are non-Raman-active	16
iii. Analyte enrichment by anti-wetting SERS platforms							
Ag-decorated Si micropillar arrays ^ evaporated Ag	super-hydrophobic	rhodamine 6G (R6G) lambda DNA molecules lysozyme	aqueous aqueous aqueous	R6G: 10^{-17} M DNA: 10^{-18} M lysozyme: 10^{-15} M	lysozyme: 1.5×10^{6}	analyte concentration factor $>10^4$	17
Ag-coated natural taro-leaf ^ evaporated Ag	super-hydrophobic	rhodamine 6G (R6G)	aqueous	10^{-8} M	10^{6}	analyte concentration factor >43	38
Array of Ag nanocubes assembled using Langmuir-Blodgett technique ^ Ag nanocube	super-hydrophobic	rhodamine 6G (R6G)	aqueous	10^{-16} M (10^{-10} M)	10^{11} *AEF	analyte concentration factor ~9	37
3D Ag nanowire mesh-like array ^ Ag nanowire	super-hydrophobic and oleophobic	melamine sudan I	aqueous toluene	melamine: 10^{-10} M (10^{-10} M) sudan I: 10^{-10} M (10^{-7} M)	melamine: 1.8×10^{11} sudan I: 1.9×10^{8} *AEF	analyte concentration factor ~100 for aqueous-based solution ~10 for toluene-based solution	10
Slippery liquid-infused porous SERS (SLIPSERS) ^ Au nanoparticle	non-stick surfaces	rhodamine 6G thymine adenine bovine serum albumin (BSA) bis(2-ethylhexyl) phthalate (DEHP) Polychlorinated biphenyl 7 (PCB 7) PCB 209	aqueous/ethanol aqueous aqueous aqueous ethanol acetone acetone	R6G: 10^{-18} M (10^{-13} M) thymine: 10^{-17} M adenine: 10^{-17} M BSA: 10^{-17} M DEHP: 10^{-17} M PCB 7: 2.3×10^{-10} M PCB 209: 10^{-10} M	N.A.	N.A.	18
iv. Molecule enrichment by functionalizing SERS platforms with porous materials							
Au superparticle (GSP)@zeolitic imidazolate framework-8 ^ Au nanoparticle	MOF	4-ethylbenzaldehyde	volatile organic compound (VOC)	10^{-8} v/v (10^{-8} v/v)	N.A.	~1.5-fold signal enhancement over bare GSP substrates	8
MOF-encapsulated Ag film-over-nanosphere ^ evaporated Ag	MOF	toluene benzene pyridine nitrobenzene 2,6-di-*tert*-butylpyridine	VOC VOC VOC VOC VOC	benzene: 8×10^{-6}	N.A.	N.A.	39
MOF-encapsulated Ag nanocube array (plasmonic nose) ^ Ag nanocube	MOF	4-methylbenzenethiol (MBT) toluene 2-naphthalenethiol (NT)	VOC VOC VOC	toluene: 8×10^{-6} M (8×10^{-6} M) NT: 2×10^{-9} M	MBT: 7.6×10^{6} toluene: 2×10^{5} *AEF	>2-fold higher AEF and sorption rate constant compared to bare SERS platform	11

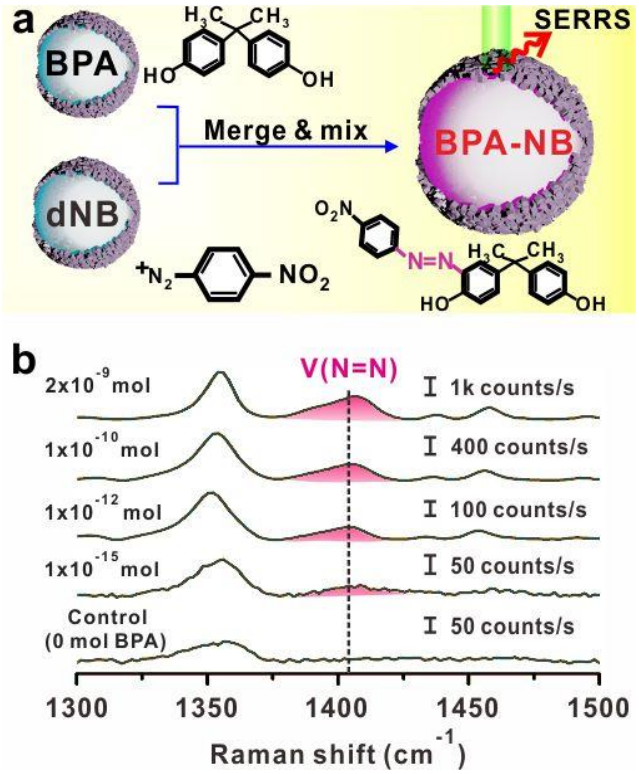

Figure 5. Enlarging analyte's Raman cross-section though chemical modification. (a) Scheme illustrating the azo coupling of bisphenol A (BPA) with diazonium cation to yield BPA-derived azo dye. This allows the (b) ultrasensitive SE(R)RS detection of BPA down to 10 amol. Reprinted and adapted with permission from ref 19. Copyright 2017 American Chemical Society.

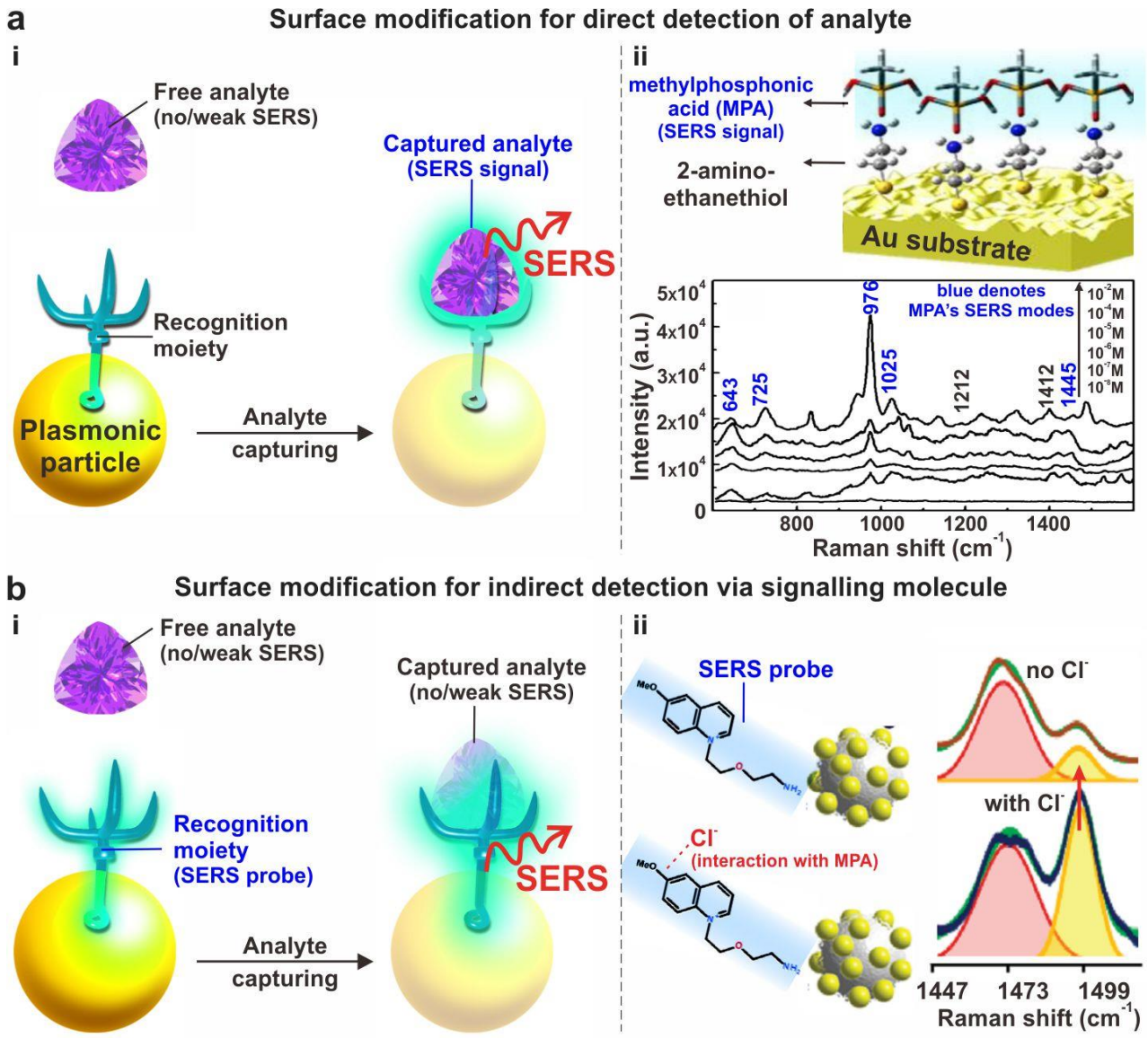

Figure 6. Direct and indirect SERS detections using analyte directing strategies. (a) Direct SERS detection of analyte. (i) Scheme depicting the working principle of direct SERS detection. (ii) Using surface-grafted 2-aminoethanethiol to capture target methylphosphonic acid (MPA) molecules for ultrasensitive MPA detection (top). Corresponding SERS spectra of MPA at varying concentrations between 10^{-2} and 10^{-8} M (bottom). (b) Indirect SERS detection of analyte. (i) Working principle of indirect SERS detection. (ii) Schematic representation of indirect chloride detection (left). Magnified SERS spectra showing the change in 1472 and 1497 cm^{-1} SERS bands upon chloride interaction with the surface-grafted SERS label (right). Reprinted and adapted with permission from (a-ii) ref 34 and (b-ii) 16. Copyright 2017 Elsevier. Copyright 2011 American Chemical Society.

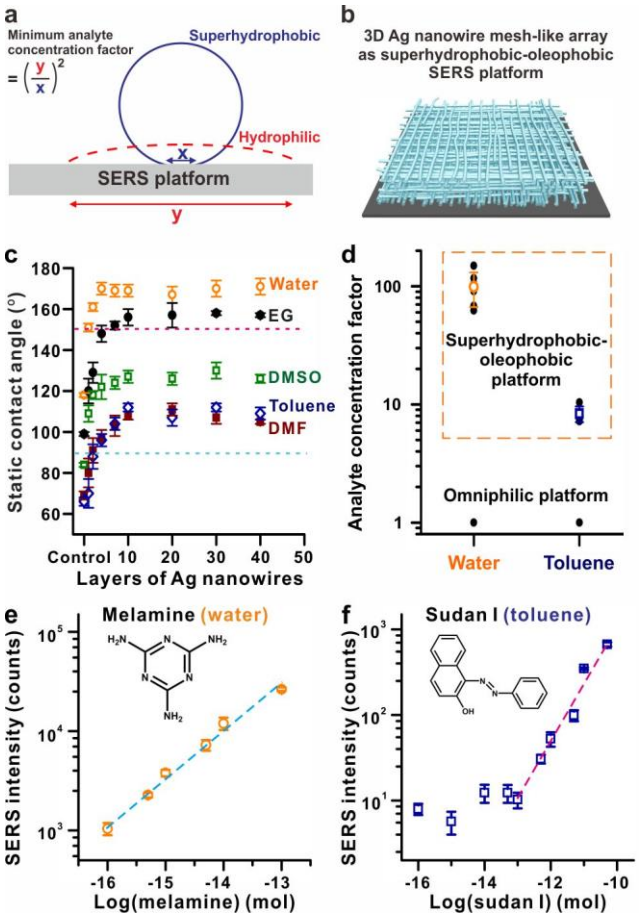

Figure 7. Using non-wetting phenomena to concentrate analyte molecules within the SERS-active region. (a) Scheme explaining the analyte concentrating mechanism using superhydrophobic platform as an example. (b) Scheme of superhydrophobic-oleophobic (SHP-OP) SERS-active Ag nanowire mesh-like array. (c) Static contact angle of various liquids of SERS platforms created from different layers of Ag nanowires. (d) Comparison of analyte-concentration factor of SHP-OP platform with an omniphilic platform. SERS intensities of (e) melamine and (f) sudan I as a function of their concentrations. Reprinted and adapted with permission from ref 10. Copyright 2014 American Chemical Society.

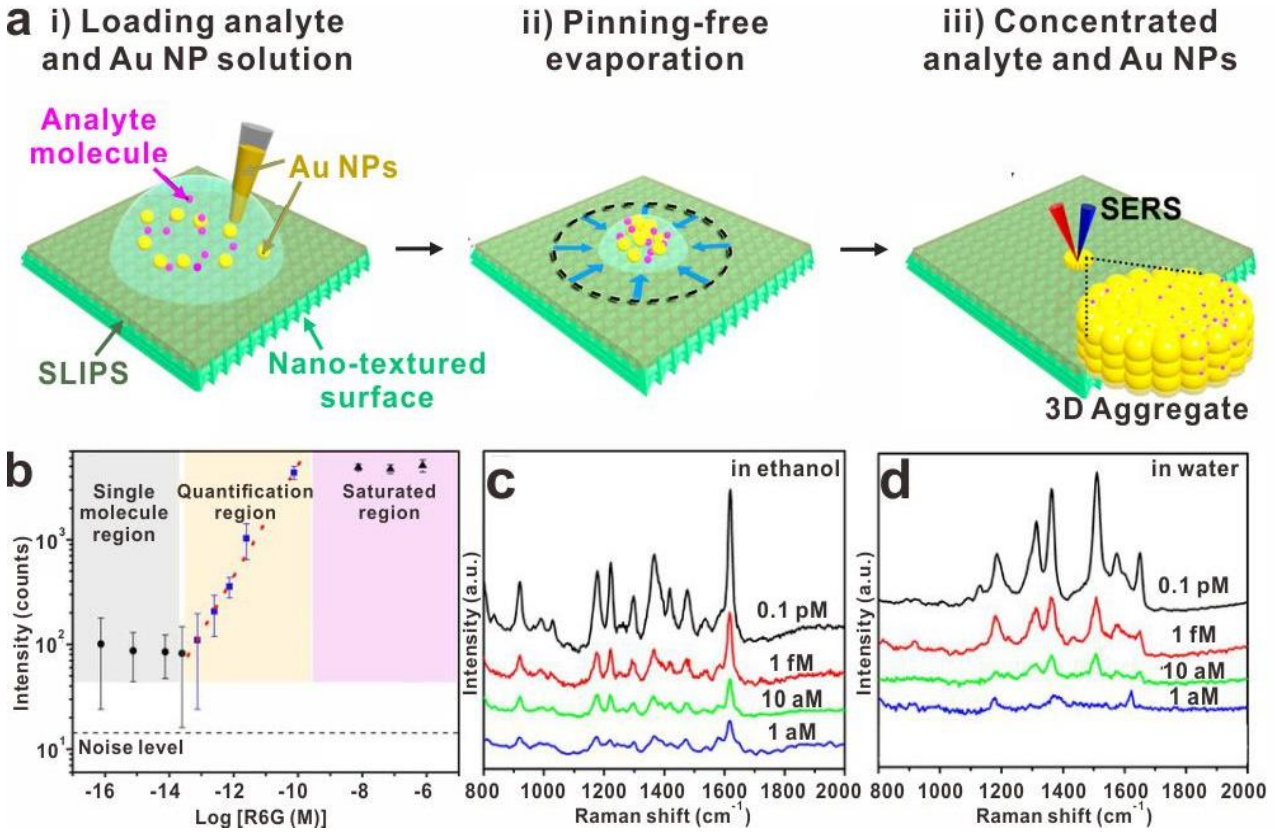

Figure 8. Slippery liquid-infused porous SERS (SLIPSERS). (a) Scheme depicting the SLIPSERS concept to enrich any analyte from common fluids. SLIPS refers to slippery liquid-infused porous substrate. (b) SERS intensity at 1,362 cm^{-1} as a function of R6G concentrations. (c) SERS spectra of R6G molecules obtained from ethanol solutions at different concentrations. (d) SERS spectra of R6G molecules obtained from aqueous solutions at different concentrations. Reprinted and adapted with permission from ref 18. Copyright 2016 National Academy of Sciences.

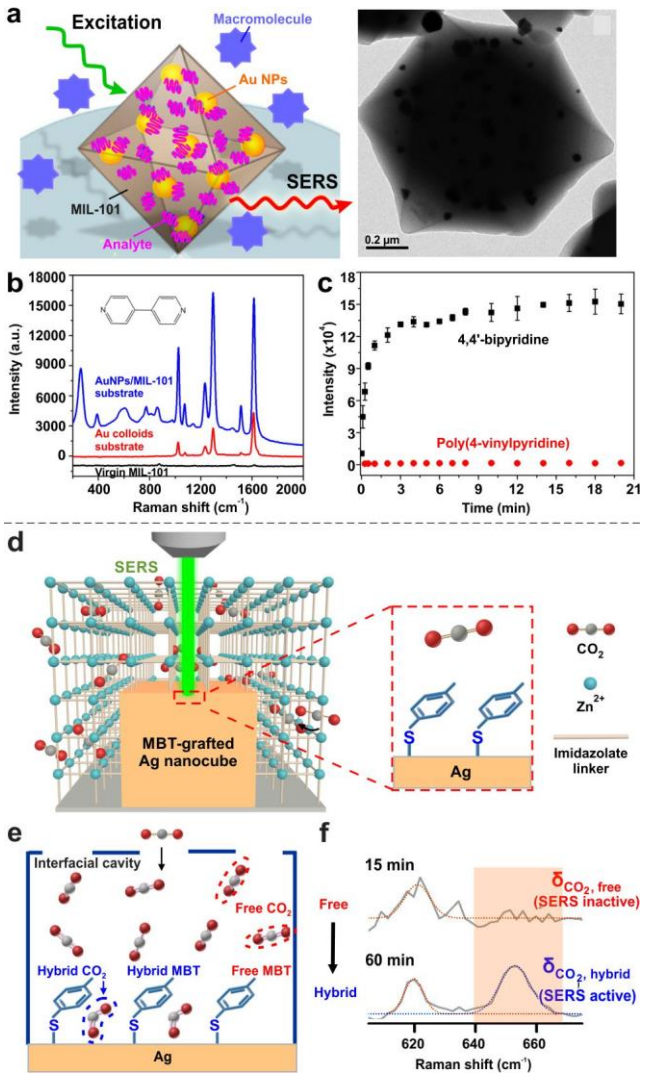

Figure 9. Metal-organic framework (MOF)-assisted selective concentration of analytes onto nanoparticle surfaces for ultrasensitive SERS application. (a) Scheme illustrating the selective concentration of analyte on plasmonic surfaces using AuNPs/MIL-101 ensemble (left). TEM image of as-synthesized AuNPs/MIL-101 (right). (b) SERS spectra of 4,4-bipyridine on AuNPs/MIL-101 substrate (blue), Au colloids substrate (red) and virgin MIL-101 (black). (c) Raman intensity plotted against time at 1030 and 1292 cm^{-1} for 0.64 μmol/L 4,4′-bipyridine (black square) and poly(4-vinylpyridine) (red circle), respectively. (d) Scheme illustrating the use of MOF-encapsulated Ag nanocube to track solid-gas dynamic using SERS. (e) Temporal SERS monitoring unravels the formation of pseudo high-pressure CO_2 microenvironment on the Ag surfaces. This is affirmed from the (f) evolution of CO_2 bending vibrational mode which is SERS-active only in bent CO_2 molecular configuration. Reprinted and adapted with permission from (a-c) ref 41 and (d-f) ref 42. Copyright 2014 and 2017 American Chemical Society.

Table 3: Design and application of SERS platforms beyond hotspot engineering – Emerging hybrid SERS platforms.

SERS platform ^ Plasmonic building block	Approach	Analyte(s)	Analyte medium	Limit of detection (Limit of quantification)	Enhancement factor (EF)/ Analytical enhancement factor (AEF)	Comments	Ref
Emerging hybrid SERS platform (plasmonic platform + 2D / semi-conductor / stimuli-responsive materials)							
Ag octahedron@graphene oxide ^ Ag octahedron	hybrid/ graphene oxide	4-aminothiophenol (ATP) 4-methylbenzenethiol (MBT) 4-methylbenzoic acid (MBA) rhodamine 6G (R6G) crystal violet (CV)	ethanol ethanol ethanol ethanol ethanol	R6G: 10^{-10} M (10^{-10} M) CV: 10^{-9} M (10^{-9} M)	ATP: 9.8×10^{5} MBT: 9.2×10^{5} MBA: 8.6×10^{5} *single particle level	>2-fold enhanced SERS intensity compared to pure Ag nanoparticle	20
Zinc oxide nanofibers deposited on a Ag foil surface ^ Ag foil	hybrid/zinc oxide	4-aminothiophenol (ATP)	aqueous	10^{-12} M	1.2×10^{8}	N.A.	48
Photo-induced enhanced Raman spectroscopy (PIERS) substrate ^ Au nanoparticle, Ag nanoparticle	hybrid/TiO_2	rhodamine 6G (R6G) dinitrotoluene (DNT) trinitrotoluene (TNT) cyclotrimethylenetrinitramine (RDX) pentaerythritol tetranitrate (PETN) glucose	methanol methanol methanol / VOC methanol methanol aqueous	R6G: 10^{-7} M DNT: 10^{-15} M TNT: 10^{-5} M RDX: 10^{-5} M PETN: 10^{-5} M glucose: 10^{-9} M	R6G: 1.3×10^{8} DNT: 5.2×10^{9} TNT: 1.1×10^{6} RDX: 1.1×10^{6} PETN: 9.0×10^{5} glucose: 1.7×10^{10} *AEF	additional enhancement from PIERS: PIERS / SERS = 4.2 (R6G) = 3.8 (DNT) = 4.1 (TNT) = 20.3 (RDX) = 6.0 (PETN) = 34.8 (glucose)	12
Au-TiO_2 nanocomposite ^ Au nanoparticle	hybrid/TiO_2	4-mercaptobenzoic aicd	ethanol	10^{-8} M	7×10^{3}	N.A.	49
Graphene oxide (GO) attached to nanopopcorn ^ Au nanopopcorn	hybrid/ graphene oxide	rhodamine 6G methicillin-resistant *Staphylococcus Aureus* (MRSA)	N.A. N.A.	R6G: 10^{-10} M MRSA: 10 CFU/mL	R6G: 3.8×10^{11}	$>10^{2}$ better than bare Au nanopopcorn	21

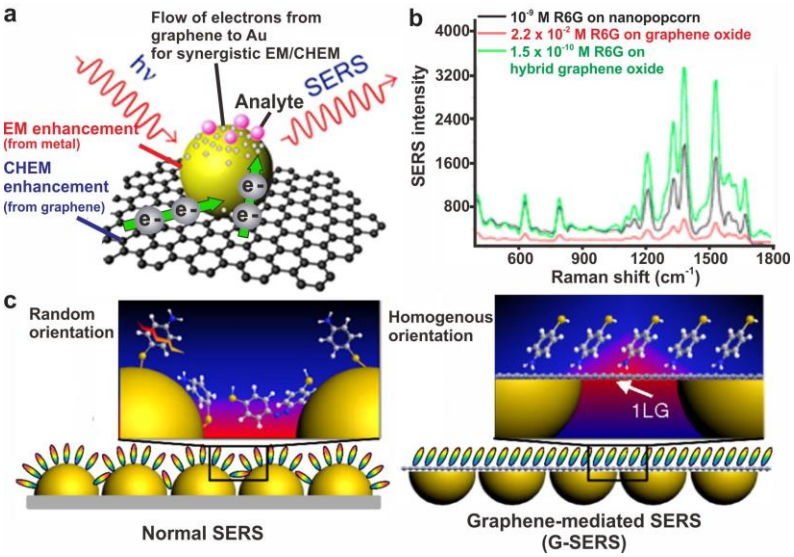

Figure 10. Graphene/metal hybrid SERS structures. (a) Scheme of EM and CHEM enhancements of analyte molecules adsorbed on AuNP/graphene SERS substrate. (b) Comparisons of Raman spectra for R6G at 785 nm excitation using Au nanopopcorn-attached graphene oxide hybrid (green), graphene oxide (red) and Au nanopopcorn (black). (c) Schematic illustration of molecules adsorbed on a normal SERS substrate (left) and on a G-SERS substrate (right). Reprinted and adapted with permission from (a) ref 45, (b) ref 21 and (c) 47. Copyright 2013 Elsevier. Copyright 2013 American Chemical Society. Copyright 2012 National Academy of Sciences.

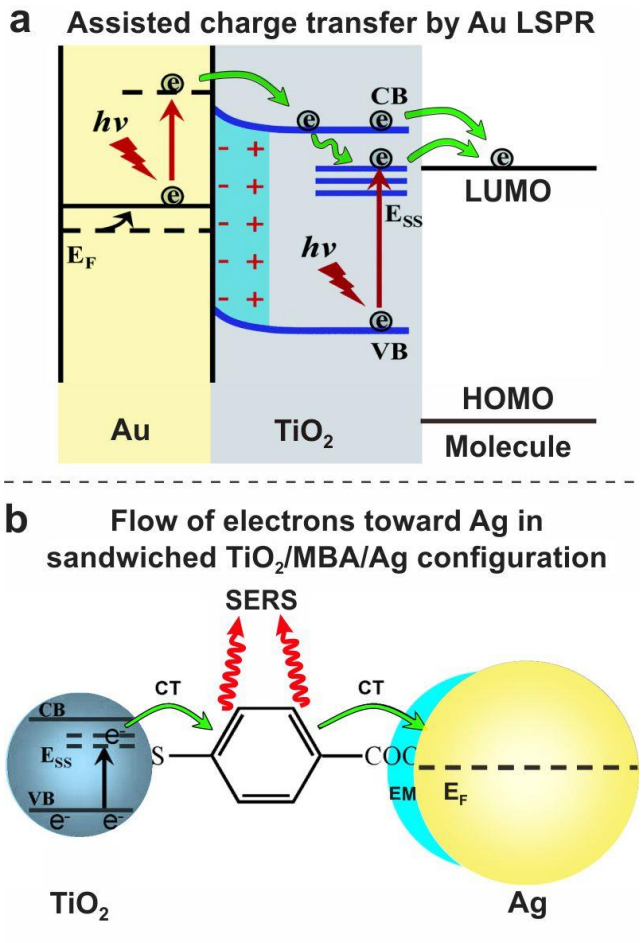

Figure 11. Synergistic chemical enhancement of semiconductor/metal hybrid SERS structures. (a) SERS enhancement mechanism of 4-MBA adsorbed on Au–TiO_2. (b) Charge transfer mechanism associated with a sandwiched TiO_2/MBA/Ag configuration. Reprinted and adapted with permission from (a) ref 49 and (b) ref 50. Copyright 2017 Royal Society of Chemistry. Copyright 2012 American Chemical Society.

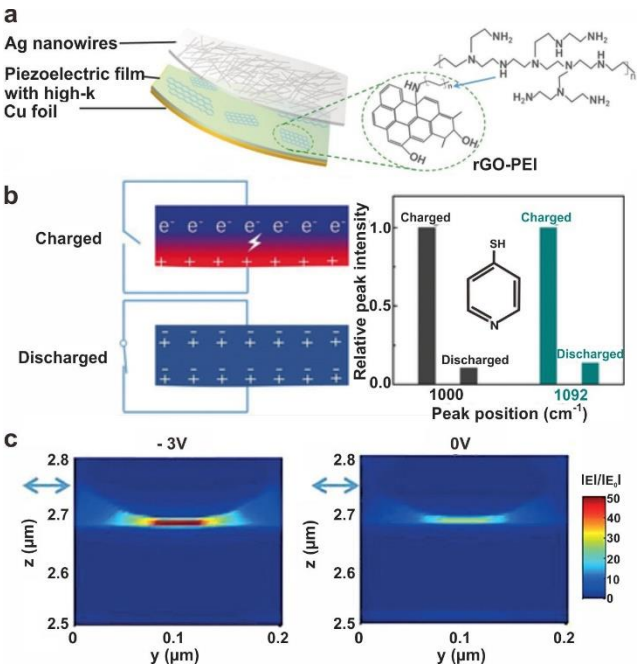

Figure 12. Piezoelectric materials for hybrid SERS structures. (a) Schematic illustration of the piezo E-SERS-active device. (b) Schematic illustration of the charged and discharged states of the device and the measured Raman intensities during these states. (c) Electromagnetic field intensity distribution in the monitor window around the hotspot, with varying underlining electric potential of -3 V and 0 V. Reprinted and adapted with permission from ref 43. Copyright 2017 John Wiley & Sons, Ltd.

Biographies

Ling's group was established in Nanyang Technological University (NTU), Singapore, in 2011. The research programs in our laboratory combine chemistry, nanotechnology, and materials science approaches to develop functional nanostructures with novel catalysis, plasmonic, sensing, and anti-counterfeiting applications. Our research activities involve nanoparticle synthesis, surface chemistry, self-assembly, nanopatterning, nanofabrication, materials and device characterization, as well as subsequent applications of our unique SERS platforms for ultrasensitive molecular detections. Chee Leng Lay is an A*STAR scholar and is currently pursuing her Ph.D. in Chemistry at NTU, working on SERS-based anti-counterfeiting applications and stimuli-responsive materials. Howard Yi Fan Sim is a Ph.D. student in NTU and is working on MOF-SERS platform for in situ monitoring of chemical reactions. Ya-Chuan Kao is also a Ph.D. student in NTU and his research focuses on fabricating superhydrophobic SERS substrates for biosensing. Qi An is an Associate Professor in China University of Geosciences and is currently a visiting scholar in NTU, researching on layer-by-layer material for biochemistry and piezoelectric SERS devices.

Hiang Kwee Lee received his Bachelor's degree in Chemistry and Biological Chemistry from Nanyang Technological University (2013), Singapore. He was an A*STAR scholar and received his Ph.D. in Chemistry at Nanyang Technological University (2018), under the supervision of Prof. Xing Yi Ling and Dr. In Yee Phang (A*STAR). He is currently a research fellow under the guidance of Prof. Xing Yi Ling. His research interests include the fabrication of superhydrophobic SERS substrate, assembly of 2D and 3D substrateless SERS platforms, and their applications for toxin sensing, reaction modulation and in situ process monitoring.

Yih Hong Lee received his Ph.D. in Chemistry from National University of Singapore (2012). He is currently a senior research fellow under the guidance of Prof. Xing Yi Ling. His research interests include nanoparticle self-assembly, plasmonics, and optical behaviors of two-dimensional transition dichalcogenides. In nanoparticle self-assembly, he is interested in using nanoscale surface chemistry to direct the organization of nanoparticles into distinct metacrystals and their applications as substrate-less sensing platforms.

Charlynn Sher Lin Koh received her Bachelor's degree in Chemistry and Biological Chemistry from Nanyang Technological University (2016), Singapore. She was awarded the Nanyang President's Graduate Scholarship and is currently pursuing her Ph.D. in nanomaterial chemistry at Nanyang Technological University. Her research interests include the use of substrateless 2D and 3D platforms in multifunctional applications such as in situ electrochemical-SERS investigation and molecular-level gas sensing.

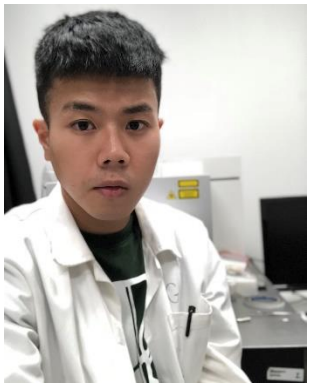

Gia Chuong Phan-Quang received his Bachelor's degree in Chemistry and Biological Chemistry from Nanyang Technological University (2015), Singapore. He was awarded the Nanyang President's Graduate Scholarship and is pursuing a Ph.D. degree in the same department, under the supervision of Prof. Xing Yi Ling. Chuong is currently researching on plasmonic colloidosomes, 3D SERS platforms and their applications for detection and in situ reaction screening at the picoliter scale.

Xuemei Han received her Ph.D. in Chemistry from the Technical Institute of Physics and Chemistry, University of Chinese Academy of Science (2012). She worked as a postdoctoral fellow in the Department of Chemistry and Biological Chemistry at Nanyang Technological University in Prof. Xing Yi Ling's lab. Her current research interests focus on developing ultrasensitive SERS sensors and their subsequent integration with chemometric analyzing method for the detection of disease-related biomarker in complex biofluids.

Xing Yi Ling obtained her Ph.D. from University of Twente (2008), the Netherlands, under the supervision of Prof. David Reinhoudt and Prof. Jurriaan Huskens. She did her postdoctoral research in Prof. Peidong Yang's group at the University of California, Berkeley, with the Rubicon fellowship from The Netherlands Organization for Scientific Research. She joined NTU in 2011 and obtained her tenured associate professorship in 2016. She is the recipient of IUPAC Young Chemist award (2009), Singapore National Research Foundation fellowship (2012), Asian and Oceanian Photochemistry Association prize for Young Scientist (2014), and L'ORÉAL Singapore for Women in Science National Fellowships (2015).